Mapping the membrane topography of the TH6–TH7 segment of the diphtheria toxin T-domain channel

Paul K. Kienker,[1] Zhengyan Wu,[1] and Alan Finkelstein[1,2]

[1]Department of Physiology and Biophysics, and [2]Department of Neuroscience, Albert Einstein College of Medicine, Bronx, NY 10461

Low pH triggers the translocation domain of diphtheria toxin (T-domain), which contains 10 α helices, to insert into a planar lipid bilayer membrane, form a transmembrane channel, and translocate the attached catalytic domain across the membrane. Three T-domain helices, corresponding to TH5, TH8, and TH9 in the aqueous crystal structure, form transmembrane segments in the open-channel state; the amino-terminal region, TH1–TH4, translocates across the membrane to the trans side. Residues near either end of the TH6–TH7 segment are not translocated, remaining on the cis side of the membrane; because the intervening 25-residue sequence is too short to form a transmembrane α-helical hairpin, it was concluded that the TH6–TH7 segment resides at the cis interface. Now we have examined this segment further, using the substituted-cysteine accessibility method. We constructed a series of 18 mutant T-domains with single cysteine residues at positions in TH6–TH7, monitored their channel formation in planar lipid bilayers, and probed for an effect of thiol-specific reagents on the channel conductance. For 10 of the mutants, the reagent caused a change in the single-channel conductance, indicating that the introduced cysteine residue was exposed within the channel lumen. For several of these mutants, we verified that the reactions occurred primarily in the open state, rather than in the flicker-closed state. We also established that blocking of the channel by an amino-terminal hexahistidine tag could protect mutants from reaction. Finally, we compared the reaction rates of reagent added to the cis and trans sides to quantify the residue's accessibility from either side. This analysis revealed abrupt changes in cis- versus trans-side accessibility, suggesting that the TH6–TH7 segment forms a constriction that occupies a small portion of the total channel length. We also determined that this constriction is located near the middle of the TH8 helix.

The Journal of General Physiology

INTRODUCTION

Diphtheria toxin (DT) is a 535-residue protein with three domains: a carboxy-terminal receptor-binding domain, a central translocation or transmembrane domain (T-domain), and an amino-terminal catalytic domain. In the aqueous crystal structure of the toxin, the T-domain contains 10 α helices, designated TH1–TH5, TH5′, and TH6–TH9 (Bennett et al., 1994). After the toxin binds to a receptor on the surface of its target cell, it undergoes endocytosis and reaches an acidic vesicle compartment. Here, the T-domain senses the low pH, changes its conformation to insert into the endosomal membrane, and translocates the catalytic domain across the membrane to the cytosol, where it acts as a lethal enzyme (see Murphy, 2011). Translocation of the catalytic domain and helices TH1–TH4 of the T-domain has also been demonstrated using purified protein in planar phospholipid bilayer membranes (Senzel et al., 1998, 2000; Oh et al., 1999b). Whole DT or its B_{45} fragment (roughly equivalent to the T-domain) added to the cis side of such membranes forms transmembrane channels, whose formation is promoted by a low pH on the cis side and a higher pH on the opposite, trans, side (Donovan et al., 1981; Kagan et al., 1981). It is widely accepted that channel formation is a necessary condition for translocation of the catalytic domain, although the precise connection between the two has not been determined (Murphy, 2011).

Knowledge of the T-domain channel's structure might help us to understand how it enables the translocation of the catalytic domain. Thus far, however, a comprehensive structural picture has been elusive. Part of the problem may be that the T-domain can assume a variety of channel and nonchannel structures in the membrane (Rosconi and London, 2002). To some extent, this can be addressed by studies of the open-channel state in planar bilayers. A more vexing problem is how to reconcile three seemingly contradictory observations:

Correspondence to Paul K. Kienker: paul.kienker@einstein.yu.edu

Z. Wu's present address is Key Laboratory of Ion Beam Bioengineering, Hefei Institutes of Physical Science, Chinese Academy of Sciences, Hefei, 230031 Anhui, China.

Abbreviations used in this paper: AChR, acetylcholine receptor; DT, diphtheria toxin; His_6-tag, hexahistidine tag; MTS-ACE, [2-(aminocarbonyl)ethyl] MTS; MTS-EA, 2-aminoethyl MTS hydrobromide; MTS-EH, 2-hydroxyethyl MTS; MTS-ET, [2-(trimethylammonium)ethyl] MTS bromide; MTS-glucose, *N*-(β-D-glucopyranosyl)-*N*′-[(2-methanethiosulfonyl)ethyl] urea; pCMBS, 4-(chloromercuri)benzenesulfonic acid sodium salt; SCAM, substituted-cysteine accessibility method; T-domain, translocation domain of DT.

The Rockefeller University Press $30.00
J. Gen. Physiol. Vol. 145 No. 2 107–125
www.jgp.org/cgi/doi/10.1085/jgp.201411326

the channel has a large diameter (Hoch et al., 1985), but it is formed by a monomer of T-domain (Gordon and Finkelstein, 2001), and it has only three transmembrane segments (Senzel et al., 2000). An earlier study showed that TH5, TH8, and TH9 are transmembrane segments in the open-channel state, with TH1–TH4 located on the trans side (Senzel et al., 2000) (Fig. 1). Residues 294 and 320 were located on the cis side, and so the intervening 25-residue segment (roughly corresponding to TH6–TH7) (Fig. 1, inset), too short to form a transmembrane α-helical hairpin, was assumed to lie on the cis side. There is some evidence, however, that the TH6–TH7 segment can insert into the membrane without spanning it (Rosconi and London, 2002). In this paper, we examine the TH6–TH7 segment more carefully to see if it may be an intrinsic part of the channel.

Our approach was to use the substituted-cysteine accessibility method (SCAM) (Karlin and Akabas, 1998). In this method, a series of mutant T-domains, each with a single cysteine residue introduced in the TH6–TH7 segment, was prepared. Each mutant T-domain was then allowed to form channels in a planar bilayer and was probed with a membrane-impermeant, thiol-specific reagent. If reaction with the cysteine occurred and caused a change in the channel conductance, this indicated that the cysteine was exposed within the channel. We performed further experiments to check that the reactions actually occurred in the open state of the channel. Additional information about the location of the cysteine was available by comparing the reaction rate of cis-side reagent to that of trans-side reagent (Wilson and Karlin, 1998; Karlin, 2001).

MATERIALS AND METHODS

Mutagenesis and protein preparation

Cloning, expression, and protein purification of the T-domain constructs were performed as described previously (Zhan et al., 1995), with induction at 30°C. Site-directed mutagenesis was done using the QuikChange Site-Directed Mutagenesis kit (Agilent Technologies). The T-domain (residues 202–378 of DT) contains no natural cysteines. The expressed proteins contained an amino-terminal hexahistidine tag (His_6-tag) with the sequence Gly-Ser-Ser-$(His)_6$-Ser-Ser-Gly-Leu-Val-Pro-Arg-Gly-Ser-His-Met. (As shown by Senzel et al., 1998, the amino-terminal methionine encoded in the plasmid construct is removed during expression.) For the most part, we kept the His_6-tag, but in some cases it was removed by thrombin cleavage, leaving the four residues Gly-Ser-His-Met at the amino terminus. In either case, we use the standard residue numbers derived from native DT (Greenfield et al., 1983). The sites at which cysteine mutagenesis was performed in this study were residues 300–317, inclusive, in the TH6–TH7 region. Mutants in the TH8–TH9 segment were the same samples described by Huynh et al. (1997).

Mutant proteins at concentrations of ∼1 mg/ml were stored at −80 or −20°C in 20 mM Tris, pH 8.0, with 2 mM dithiothreitol (DTT). Before use, a thawed aliquot was incubated with 10 mM DTT for 5 min at room temperature to ensure reduction of the cysteine residue. Concentrated protein solutions and 10-fold dilutions could undergo numerous freeze–thaw cycles while still retaining channel-forming activity; more dilute solutions were discarded at the end of the day. DTT solutions were prepared daily from 1 M stock, which was stored at −20°C.

Planar bilayer experiments

Planar bilayers were formed by the Montal–Mueller technique (Montal, 1974) across a small aperture in a partition separating two compartments, designated "cis" and "trans." Two types of chamber were used, with the compartments separated either by a 50-μm-thick Teflon partition, as described in Kienker et al. (2000), or by the side of a polystyrene "cup" (Wonderlin et al., 1990) that formed one of the compartments, as described in Silverman et al. (1994). The volume of each compartment was ∼1 ml, except for that of the inside of the cup, which was 0.5 ml. Pretreatment with solutions of squalene and asolectin was as described in the respective references for each chamber type. Similar results were obtained with either type of chamber, but the cup setup allowed for recording with lower noise and higher time resolution. The aperture diameter was ∼50–120 μm, except as discussed below. The bathing solution was 1 M KCl, 2 mM $CaCl_2$, 1 mM EDTA, and an appropriate buffer, which was typically 20 mM malic acid, pH 5.3, in the cis compartment and 20 mM HEPES, pH 7.2, in the trans compartment. In some experiments, the cis pH was raised after channel formation so that the MTS reaction would be faster; in this case, the cis buffer was typically 5 mM MES, pH 5.3, and concentrated HEPES buffer solution was added to raise the cis pH. We used a variety of pH conditions as needed to obtain good channel activity and reasonably fast reactions.

Voltage-clamp recording was performed with three different setups: an EPC7 patch-clamp amplifier (List-Medical) (Silverman et al., 1994), a homemade current to voltage converter with an OPA102 operational amplifier (Burr-Brown) (Kienker et al., 2000), or a third recording setup. This third setup used a BC-525C Bilayer Clamp amplifier (Warner Instruments), an LPF-8 low-pass Bessel filter (Warner Instruments), and an NI USB-6211 A/D converter (National Instruments). The program IgorPro (6.2.4.1) with the NIDAQ Tools MX package (1.0.5.4; WaveMetrics) was used for data acquisition and analysis. In all cases, the voltage is defined as the potential of the cis compartment (the compartment to which the T-domain was added) relative to that of the trans compartment. Low-pass filtering was typically 30 Hz for macroscopic experiments and 5–30 Hz for single-channel experiments. Single-channel experiments at higher time resolution (1,000 Hz) used cup chambers as in Silverman et al. (1994), except that the apertures were smaller (20–30-μm diameter) and slightly smaller amounts of lipid and squalene solutions were applied to the aperture to avoid clogging.

The MTS reagents used were [2-(trimethylammonium)ethyl] MTS bromide (MTS-ET), 2-aminoethyl MTS hydrobromide (MTS-EA; Biotium), [2-(aminocarbonyl)ethyl] MTS (MTS-ACE), and *N*-(β-D-glucopyranosyl)-*N*′-[(2-methanethiosulfonyl)ethyl] urea (MTS-glucose; Toronto Research Chemicals). MTS stock solutions were typically 20 mg/ml in water and were stored at −20°C. More concentrated stock solutions were sometimes used: ∼200 mg/ml MTS-ET and 40 mg/ml MTS-ACE. At this concentration, the MTS-ACE would often come out of solution after freezing and thawing but could be easily re-dissolved. Typically, MTS reagents were added to a concentration of ∼1 mM, although concentrations from 7 μM to 11 mM were used on occasion.

Another thiol-specific reagent, 4-(chloromercuri)benzenesulfonic acid sodium salt (pCMBS; Toronto Research Chemicals) was prepared as a 6.5-mg/ml stock solution in water, stored at −20°C, and used within 2 d, typically at concentrations of 0.2–0.8 mM.

Data analysis

In macroscopic experiments with mutant T-domain channels, the addition of an MTS reagent typically produced a relatively fast decrease in membrane current amplitude, with approximately

exponential kinetics, and in some cases a subsequent slower decrease. We provisionally attribute the faster effect to a decrease in single-channel conductance whose kinetics reflect the reaction rate, and ascribe the slower effect to channel gating or other events that occur after the reaction. For instance, reagent added to the cis compartment could react with T-domain in solution, leading to loss of channels from the membrane, which we refer to as a "washout" effect. (This could occur if there is a dynamic equilibrium between protein in solution and channels in the membrane, and MTS reaction in solution prevents the insertion of new channels into the membrane.)

Based on this view, we used the following procedure for estimating reaction rate constants from macroscopic experiments. If a reaction beginning at time t = 0 changes the membrane current I(t) from I_0 to I_∞ with single-exponential kinetics, that is, $I(t) = I_\infty + (I_0 - I_\infty)\exp(-k_1 t)$, then it follows that the (pseudo-first order) reaction rate constant k_1 is given by

$$k_1 = \frac{\left[\left(-\frac{dI}{dt}\right)\Big/ I_0\right]}{(I_0 - I_\infty)/I_0}, \tag{1a}$$

with dI/dt evaluated at t = 0. The numerator is the magnitude of the initial slope of the normalized current trace, and the denominator is the fractional change in current over the course of the reaction. For mutant channels responsive to both cis and trans MTS reagent, we supposed that at least the initial part of the response arises primarily from a single-channel conductance change, whose magnitude is the same regardless of the side of MTS addition. Thus, for better comparison of cis- and trans-side reaction rates, we used the same averaged denominator in both cases. (Experiments in which cis MTS caused a much larger effect than trans MTS were generally excluded from this average, on the assumption that they reflected loss of channels from the membrane.) The second-order rate constant k reported in the tables was obtained simply as

$$k = k_1/[\mathrm{MTS}]. \tag{1b}$$

In this formula, we use the bulk value of [MTS] added to the cis or trans compartment, rather than the actual (unknown) concentration at the reactive site, so k should be considered an apparent rate constant. At higher [MTS], the observed k_1 may be limited by factors other than the intrinsic reaction rate, such as the mixing time of the solutions, and it may thereby lose its dependence on [MTS]. In such a case, Eq. 1b would give a lower limit for k rather than k itself. We endeavored to exclude such high-concentration data when calculating k.

To obtain k from single-channel experiments, we determined the product $t_{adj} \equiv \Delta t \times [\mathrm{MTS}]/(1\ \mathrm{mM})$ for each observed reaction event, where Δt is the time between MTS addition and the reaction. (For channels that opened after MTS addition, Δt is the time between channel opening and the reaction.) t_{adj} is the waiting time to reaction, adjusted to reflect an MTS concentration of 1 mM. Then, for a given condition, the t_{adj} values of all the channels that reacted were averaged to produce $\tau \pm \sigma_\tau$ (mean ± SD). When we had enough data to assess the shape of the distribution of t_{adj} values, it was typically approximately exponential. The second-order rate constant k was estimated as

$$k = 1/(\tau \times 1\ \mathrm{mM}). \tag{2}$$

This is the maximum-likelihood estimate for k if a single-exponential distribution for t_{adj} is assumed.

Based on published values for other MTS reagents (Karlin and Akabas, 1998), we estimate that the uncharged MTS reagents hydrolyze with a half-time of >3 h at pH 7.0, and up to 10 times more quickly per unit increase in pH. The macroscopic and single-channel effects that we observed were much faster than this, so we used the initial [MTS] value in all calculations.

RESULTS

Initial screening of mutant T-domain channels

We prepared a series of mutant T-domain proteins with a single cysteine residue introduced from residue 300 to 317, an uncharged segment roughly corresponding to TH6–TH7 (Fig. 1, inset). All mutants showed fairly normal macroscopic (many-channel) activity in planar bilayers, with the exception of P308C and G311C, which generated noisy conductances. Most of the mutant channels had relatively normal single-channel conductances (25–50 pS in 1 M KCl, pH 5.3 cis/7.2 trans) compared with that of WT channels (≈40 pS; Huynh et al., 1997); the exception was G315C at ~75 pS. P308C and G311C channels did not stay open very well, which may account for their noisy macroscopic conductances.

T-domain with an amino-terminal His_6-tag forms channels that show rapid blocking at negative voltages and rapid unblocking at positive voltages. As previously documented, this indicates that the amino terminus has

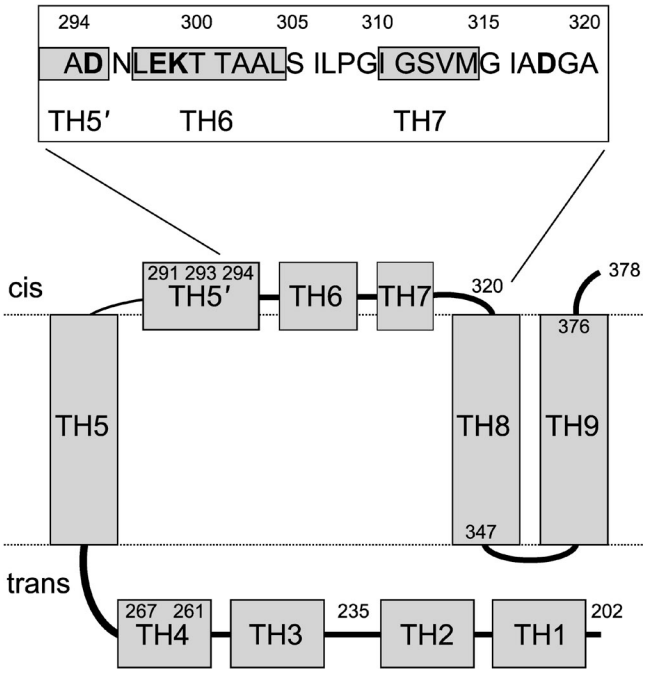

Figure 1. Previous model of the membrane topology of the T-domain in the open-channel state. The numbered residues in the main figure are those identified as being on either the cis or trans side by Senzel et al. (1998, 2000) or Gordon and Finkelstein (2001). Helices are not drawn to scale. (Inset) The amino-acid sequence of the segment from residue 294 to 320, whose ends were located on the cis side by Senzel et al. (2000). Residues with ionizable side chains are shown in bold type. The shaded boxes indicate α helices from the aqueous crystal structure (Bennett et al., 1994).

been translocated across the membrane to the trans side (Senzel et al., 1998). In our experiments, for the most part, we left the His_6-tag on the mutant T-domains so we could verify this behavior. In fact, all the mutant channels showed His_6-tag blocking with the normal voltage polarity, indicating normal translocation of the amino terminus.

Effects of MTS reagents on macroscopic conductance of TH6–TH7 mutant channels

Effects of MTS-ET. We applied SCAM (Karlin and Akabas, 1998) to the TH6–TH7 segment in the hope of identifying channel-lining residues and perhaps also learning something about the secondary structure of this segment. We began by probing each mutant channel with the positively charged thiol-specific reagent MTS-ET. (MTS-ET had no effect on WT T-domain channels.) Fig. 2 shows a representative record of a macroscopic experiment, in this case with T-domain mutant L307C and trans MTS-ET. Note the characteristic His_6-tag blocking at negative voltages and unblocking at positive voltage. We waited ~10 min for the conductance at 30 mV to stabilize, and then added MTS-ET to the trans compartment. After a short delay because of the mixing time, the conductance dropped by a small amount, indicating reaction of trans MTS-ET with the cysteine residue. This is an indication that residue 307 is exposed in the channel.

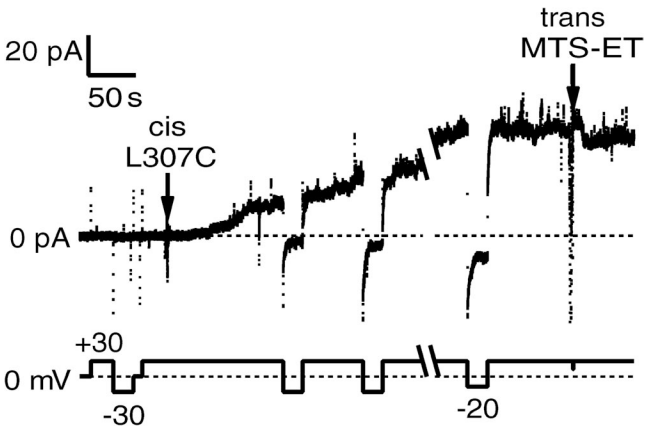

Figure 2. Effect of trans MTS-ET on T-domain mutant L307C. The top trace is current and the bottom trace is voltage, with both plotted against time. After the addition of 4 ng L307C to the cis compartment (first arrow), the current at 30 mV gradually increased as channels formed in the membrane. Upon switching to negative voltage, the magnitude of the current rapidly decreased toward zero, indicating blocking by the amino-terminal His_6-tag (Senzel et al., 1998); the current rapidly recovered upon returning to positive voltage. At the second arrow, after the channel activity had stabilized, 200 μg MTS-ET was added to the trans compartment, resulting in a decrease in current of ~19%. The solutions were 1 M KCl, 2 mM $CaCl_2$, 1 mM EDTA, with 20 mM malic acid, pH 5.3, in the cis compartment and 20 mM HEPES, pH 7.2, in the trans compartment. The break in the record was 3.6 min.

Table 1 summarizes the effects of cis and trans MTS-ET on the conductance of each mutant channel.

Exclusion of washout effects. Removal of T-domain from the cis solution by perfusion with fresh buffer leads to a slow loss of channel activity from the membrane; with our typical pH gradient of 5.3 (cis) versus 7.2 (trans), the first-order decay rate is ~0.003 s^{-1}. This can be explained if there is a dynamic equilibrium between T-domain protein in the cis solution and channels in the membrane. (Alternatively, there could be a flux of T-domain from the cis solution to open membrane channels and then to an inactive state, with the number of open channels approaching a steady state.) In principle, a cysteine mutant that cannot react with cis MTS in the open-channel state could still show an apparent effect caused by MTS reaction with T-domain in the cis solution that prevents the protein from inserting into the membrane to form a channel, thereby revealing the slow washout of channels from the membrane. Thus, a cis MTS effect as slow as the cis perfusion effect is not good evidence for reaction with the channel.

This issue can be addressed by taking measures to increase the reaction rate, such as using a higher MTS concentration or raising the pH at the reactive site. In a macroscopic experiment, raising the cis pH causes a rapid conductance increase caused by an increased single-channel conductance, followed by a slow decrease caused by loss of channel activity. If the subsequent MTS effect is much faster than this slow decrease, it can be taken as evidence for reaction with the channel in the membrane. Note that washout effects are not a concern in experiments with a membrane-impermeant MTS reagent added to the trans side, nor in single-channel experiments.

In our initial series of experiments at pH 5.3 (cis) versus 7.2 (trans), slow declines in conductance produced by 0.7 mM cis MTS-ET, which might be attributed to washout, were observed with T301C, A303C, L304C, I306C, I310C, V313C, and M314C channels. The results presented in Table 1 are based on faster effects obtained with up to 11 mM MTS-ET (for T301C, I306C, I310C, V313C, and M314C) and with an elevated cis pH (as indicated in the table).

Effects of uncharged reagents. It is possible that MTS-ET reaction with a cysteine residue near the channel entrance (within one or two Debye lengths), but not actually in the channel, could reduce the channel conductance by an electrostatic effect. This concern can be averted by the use of uncharged reagents such as MTS-ACE, which is similar in size to MTS-ET, and MTS-glucose, which is considerably larger. Because of the lower reactivity of these reagents, as compared with that of MTS-ET, many of the effects that we observed were slow enough that the possibility of a washout effect was a concern.

We did, however, see reasonably fast effects with cis and trans MTS-ACE for S305C (a decrease of ~65%) and with trans MTS-glucose for L307C and G309C channels (decreases of 22 and 19%, respectively) at pH 5.3 (cis) versus 7.2 (trans). (Cis MTS-glucose had no effect on G309C; it caused a slow decrease in conductance for L307C that could have been a washout effect.)

Single-channel results

Effects of MTS reagents on single-channel conductance. The mutants that showed a macroscopic effect of MTS-ET were also examined at the single-channel level. 10 of the mutants showed a change in single-channel conductance upon reaction (Table 1). We also observed single-channel conductance changes upon reaction with uncharged MTS reagents for seven of these mutants (Table 2). (We have not counted the −100% entries in Tables 1 and 2, as it is likely that these result from channel closure rather than from a change in single-channel conductance.)

For I310C, with the cis pH raised to 6.2–6.7 after channel formation, cis MTS-ET caused an increase in channel flickering, with the probability of the closed state increasing ~10-fold, from 7 to 71%; however, the open-channel conductance did not change. (Note that in preliminary experiments with 5-Hz filtering, this erroneously appeared as a small decrease in single-channel conductance, but it was clear with 1,000-Hz filtering that the conductance did not change.) Trans MTS-ET produced a similar effect, with a longer delay before its onset.

For A303C, we observed that cis MTS-glucose caused the channels to close, but trans MTS-glucose had no effect (Table 2). (Alternatively, the effect could have been a decrease in single-channel conductance virtually to zero.) The lack of a clear change in single-channel

TABLE 1

Percent conductance change upon MTS-ET reaction with TH6–TH7 segment mutant channels

Mutant	cis MTS-ET macroscopic	trans MTS-ET macroscopic	cis MTS-ET single channel	trans MTS-ET single channel
T300C[a]	−98 ± 2 (n = 4)	NE (n = 2)	−100 ± 0 (n = 3)	ND
T301C[b]	−64 ± 4 (n = 4)	NE (n = 2)	−60 ± 3 (n = 3)	−47 ± 3 (n = 6)
A302C	−82 ± 2 (n = 2)[c]	NE (n = 2)	−73 ± 4 (n = 6)	ND
A303C[a]	−100 ± 0 (n = 3)	NE (n = 3)	ND	ND
L304C[d]	−98 ± 2 (n = 3)	NE (n = 2)	−100 ± 0 (n = 3)	ND
S305C	−71 ± 4 (n = 6)	−56 ± 6 (n = 5)	ND	−79 ± 2 (n = 7)
I306C[d]	−40 ± 18 (n = 2)	−49 ± 0 (n = 2)	−59 ± 1 (n = 3)	−63 ± 2 (n = 3)
L307C	−28 ± 4 (n = 2)	−36 ± 10 (n = 6)	ND	−70 ± 3 (n = 12)[e]
P308C[f]	Increase	Increase	ND	−16 ± 2 (n = 3)
G309C	−16 ± 6 (n = 3)	−14 ± 2 (n = 5)	ND	−31 ± 3 (n = 19)[e]
I310C	−50 ± 8 (n = 3)[b]	NE (n = 2)[b]	Flickers (n = 4)[g]	Flickers (n = 2)[g]
S312C	−75 ± 13 (n = 7)	−67 ± 18 (n = 8)	−81 ± 4 (n = 9)	−76 ± 3 (n = 3)
V313C[b]	−96 ± 4 (n = 4)	NE (n = 2)	−100 ± 0 (n = 5)	ND
M314C[b]	−96 ± 4 (n = 6)	NE (n = 4)	−39 ± 1 (n = 2)[h,i]	ND
G315C[j]	−85 ± 5 (n = 7)	NE (n = 8)	−84 ± 3 (n = 5)	−81 ± 3 (n = 3)
I316C	−98 ± 2 (n = 3)	NE (n = 2)	−100 ± 0 (n = 12)	ND
A317C[a]	−97 ± 3 (n = 3)	NE (n = 2)	−100 ± 0 (n = 4)[h]	ND

The percent conductance change is given as mean ± SD, with n being the number of macroscopic experiments or the number of single-channel reactions. All mutant channels were tested with pH 5.3 in the cis compartment and 7.2 in the trans compartment and at positive voltage (20–120 mV), except where stated otherwise. Mutants that showed no effect or a very slow effect of MTS-ET at pH 5.3/7.2 were also tested with the cis pH raised, as indicated in the table. Solutions were as in Fig. 2, except that 5 mM MES buffer was used when the cis pH was to be raised (by the addition of concentrated HEPES buffer). Mutant G311C was excluded because its noisy macroscopic conductance made it difficult to assess MTS-ET effects. NE, no effect.

[a]The cis pH was raised to 7.0–7.3 before MTS-ET addition.

[b]The cis pH was raised to 6.2–6.3 before MTS-ET addition.

[c]In macroscopic experiments with A302C at positive voltage, cis MTS-ET caused a decrease, but the conductance became noisy before the decrease had completed. The reported value is from experiments at −20 mV using A302C with the His_6-tag removed.

[d]The cis pH was raised to 6.5–6.7 before MTS-ET addition.

[e]For L307C and G309C, the single-channel conductance decrease caused by reaction with MTS-ET was larger than the corresponding macroscopic effect. This was apparently because only a fraction of the channels reacted.

[f]In macroscopic experiments with P308C (with the His_6-tag removed), both cis and trans MTS-ET caused large, gradual conductance increases on the order of 10–30-fold. In single-channel experiments, in addition to the initial small conductance decrease seen after MTS-ET addition (as shown in the table), larger conductance channels (~75 pS) were also observed.

[g]Single-channel experiments with I310C were performed with the cis pH raised to 6.2–6.7. The effect of MTS-ET was to increase the amount of channel flickering to a short-lived closed state without changing the open-channel conductance.

[h]Cis MTS-ET reaction with M314C and A317C single channels caused a large decrease in the occupancy probability of the open state.

[i]The decrease was measured with 1,000-Hz filtering.

[j]The conductance of single channels formed by G315C was abnormally high, at ~75 pS.

conductance leaves open the possibility that residue 303 is not located within the channel. Cis MTS-ET had a similar effect on the channels formed by T300C, L304C, V313C, I316C, and A317C (Table 1).

Although a full interpretation of the macroscopic and single-channel results must be deferred to the Discussion section, we can point out two salient features here. First, the periodicity characteristic of an α helix (3.6 residues) or a β sheet (two residues) is not evident in the pattern of reactive residues. Second, there may be a trend in accessibility to MTS-ET, from cis-side only (residues 302–304) to trans-exposed (residues 305–312) and back to cis-side only (residues 313–314) (Table 1). This suggests that the TH6–TH7 segment may assume some kind of hairpin structure within the membrane.

Determining the conductance state in which reaction occurs. We are trying to characterize the open-channel state of the T-domain; however, it is known that the channel makes brief (∼1-ms) sojourns to a "flicker-closed" state. Furthermore, it has been reported that for T-domain mutants with a cysteine in the TL5 loop (between TH8 and TH9), MTS reaction occurs preferentially in the flicker-closed state (Huynh et al., 1997). Thus, we needed to establish in which state reactions occur for mutants with a cysteine in the TH6–TH7 segment, using 1,000-Hz filtering so the flicker-closed state could be adequately resolved. After verifying the result of Huynh et al. (1997) that the TL5 segment mutant V351C reacts with trans MTS-EA primarily in the flicker-closed state (Table 3), we moved on to the TH6–TH7 segment. Fig. 3 shows examples of MTS reactions with single channels in the open state and in the flicker-closed state. MTS reactions occurred primarily in the open state for all of the TH6–TH7 segment mutants that we examined: T301C, S305C, L307C, G309C, and S312C (Table 3).

Effects of MTS reagents on ionic selectivity

As illustrated by the case of the I310C mutant mentioned above, an increase in channel flickering upon reaction can give the illusion of a single-channel conductance change if the flickering rate is fast compared with the low-pass filtering frequency. Although there is no particular reason to doubt the authenticity of the single-channel conductance changes that we have observed for other mutants, using 1,000-Hz filtering, they could, in principle, arise from a very fast flickering effect. Such a flickering effect cannot, however, change the ionic selectivity of the channel. Thus, for selected mutants, we examined the effect of MTS reaction on selectivity. With a salt and pH gradient of 1 M KCl, pH 5.3 (cis), versus 0.1 M KCl, pH 7.2 (trans), all of the mutants examined (301C, 302C, and 305C–315C) had reversal potentials in the range of −39 to −42 mV, comparable to the −38 to −39 mV reported for whole DT and B_{45} fragment channels under the same conditions (Mindell, 1993; Silverman et al., 1994) and indicating moderately high selectivity for K^+ over Cl^-. Upon reaction with the positively charged MTS-ET, S305C and S312C channels underwent a large decrease in cation

TABLE 2

Percent conductance change and rates of reaction for uncharged MTS reagents in single-channel experiments on TH6–TH7 segment mutant channels

Mutant	cis/trans pH	MTS reagent	Conductance change (%)	Waiting time (cis)	Waiting time (trans)	k_{cis}	k_{trans}
				s	*s*	$M^{-1}\,s^{-1}$	$M^{-1}\,s^{-1}$
T301C	6.6/7.2	Glucose	−11 ± 1 (*n* = 6)	70 ± 61 (*n* = 6)	>535[a] (*n* = 3)	14	<2
A303C	7.0/7.0	Glucose	−100 ± 0 (*n* = 10)	58 ± 33 (*n* = 10)	NE (*n* = 4)	17	NE
S305C	7.0/7.0	Glucose	−79.2 ± 0.8 (*n* = 9)	2.8 ± 2.2 (*n* = 6)	65 ± 40 (*n* = 4)	351	15
I306C	6.6/7.2	Glucose	−36 ± 2 (*n* = 3)	63 ± 43 (*n* = 8)	NE (*n* = 6)	16	NE
L307C	5.3/7.2	Glucose	−59 ± 5 (*n* = 42)	101 ± 95 (*n* = 4)	2.4 ± 2.2 (*n* = 42)	10	421
G309C	5.3/7.2	Glucose	−33 ± 4 (*n* = 55)	NE (*n* = 5)	2.4 ± 3.1 (*n* = 56)	NE	413
S312C	6.0/8.0	ACE	−33 ± 3 (*n* = 6)	54 ± 50 (*n* = 4)	18 ± 4 (*n* = 3)	18	57
"	"	Glucose	−39 ± 3 (*n* = 4)	641 ± 56 (*n* = 2)	118 ± 1 (*n* = 2)	2	8
G315C	6.0/8.0	ACE	−70 ± 1 (*n* = 5)	190 ± 89 (*n* = 2)	267 ± 136 (*n* = 3)	5	4
"	7.0/7.0	Glucose	−77 ± 3 (*n* = 3)	5.6 ± 0.6 (*n* = 3)	NE (*n* = 5)	179	NE

The percent conductance change (combining both cis and trans MTS effects) is given as mean ± SD, with *n* being the number of single-channel reactions that were used in calculating each value. Likewise, the waiting times to reaction (adjusted to reflect a 1-mM MTS concentration) are given as $\tau \pm \sigma_\tau$. Although we do not make use of the second-order rate constant, $k = 1/(\tau \times 1\ mM)$, obtained from single-channel experiments, its value is given for comparison with values in the other tables. For the most part, τ and σ_τ are approximately equal, as expected for exponentially distributed waiting times. The interested reader can estimate the SD of k as the value of k given in the table times $n/[(n-1)(n-2)^{1/2}]$, based on the assumption that the waiting times are exponentially distributed and hence the reciprocal of a sum of waiting times follows an inverse-gamma distribution (Johnson et al., 1994; Schraiber et al., 2013). The percent conductance change and waiting time could not always both be determined for a given reaction event, so the *n* values for the cis- and trans-side waiting times do not necessarily add up to the *n* value given for the conductance change. The concentrations of MTS-glucose and MTS-ACE were in the range 30 µM to 1 mM and 1 to 2 mM, respectively. NE, no effect.

[a]For T301C with trans MTS-glucose, of three channels observed, only one reacted, apparently while in a long-lived closed state, after 8–11 min. The channels that did not react were exposed to 1 mM MTS-glucose for about 10 min each.

TABLE 3

Conductance state in which MTS reaction occurred

Mutant	MTS reagent	Side of addition	Conductance change (%)	Number in open state	Number in closed state
T301C	EA	trans	−47 ± 4 (n = 6)	4	1
S305C	EA	trans	−72 ± 3 (n = 21)	25	5
L307C	EA	trans	−65 ± 2 (n = 5)	5	1
G309C	ET	trans	−30 ± 3 (n = 4)	4	0
S312C	ET	cis	−78 ± 5 (n = 2)	2	0
"	ET	trans	−75 ± 4 (n = 3)	2	1
A334C	EA	trans	−38 ± 2 (n = 11)	10	1
L338C	EA	trans	−34 ± 3 (n = 10)	15	0
V351C	EA	trans	−44 ± 9 (n = 3)	1	2

The percent conductance change is given as mean ± SD, with n being the number of single-channel reactions that were used in calculating each value. All results are from experiments with single-channel resolution. Low-pass filtering was 1,000 Hz, and the sample interval was 0.15 ms. The percent conductance change and state of reaction could not always both be determined for a given channel, so the number reacting in the open state plus that in the closed state does not necessarily add up to the n value given for the conductance change. All mutant channels were tested at positive voltage (30–120 mV) with solutions as in Fig. 2.

selectivity, with reversal potentials changing to approximately −10 and 0 mV, respectively. A302C and G315C showed more moderate effects, with reversal potentials changing to −33 and −30 mV, respectively. Hence, the MTS-ET effect on each of these mutants must be the result of an effect on the ion permeation pathway. In contrast, MTS-ET reaction had only minor effects on the selectivity of T301C, I306C, L307C, G309C, I310C, G311C, V313C, and M314C channels. This may indicate that these residues are located in a wider part of the channel or outside of the channel. (Note that we would not detect a change in selectivity if the channel closes upon, or shortly after, reaction, as we have seen for V313C and M314C, respectively; in this case, the current through unreacted channels would dominate.)

Protection from reaction by His_6-tag blocking

Segments TH1–TH4 of the T-domain, along with an introduced amino-terminal His_6-tag, are translocated across the membrane to the trans side during channel formation (Senzel et al., 1998). The His_6-tag induces channel closure at negative voltages, which is believed to represent blockade of the channel by the His_6-tag (Senzel et al., 1998). Given this picture, we thought that His_6-tag blockade might protect a cysteine residue in the channel from reaction. We performed a series of

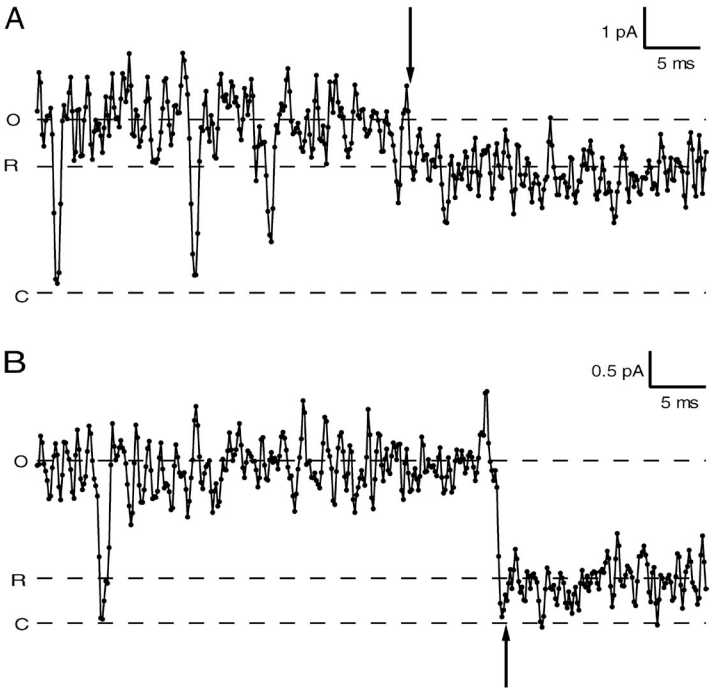

Figure 3. Single-channel recordings to determine the conductance state in which reaction occurred. Each panel shows current versus time, with the average current levels for the closed, open, and reacted states indicated by the dashed lines labeled C, O, and R, respectively. (A) About 50 min before the start of the record, 65 pg G309C was added to the cis compartment; 100 μg MTS-ET was added to the trans compartment ~15 min later. The record begins with a 43-pS channel open at 100 mV. Several brief flickers toward the closed level can be seen. A drop to the reacted level of 31 pS, marked by a downward-pointing arrow, appears to have occurred from the open state. The reaction took place ~9 s after the channel opened. (B) About 75 min before the start of the record, 180 μg MTS-EA was added to the trans compartment. Three additions of S305C totaling 18 ng were made to the cis compartment 37–73 min before the start of the record. The record begins with a 38-pS channel open at 60 mV. A brief flicker to the closed level can be seen. A drop to the reacted level of 11 pS, marked by an upward-pointing arrow, appears to have occurred via the closed state. The reaction took place ~6 s after the channel opened. For both panels, the solutions were as in Fig. 2. The filtering frequency was 1,000 Hz, and the sample interval was 0.15 ms. The current traces are shown as small closed circles connected by lines, with each circle representing one sampled data point. The zero-current level is slightly below the average closed level.

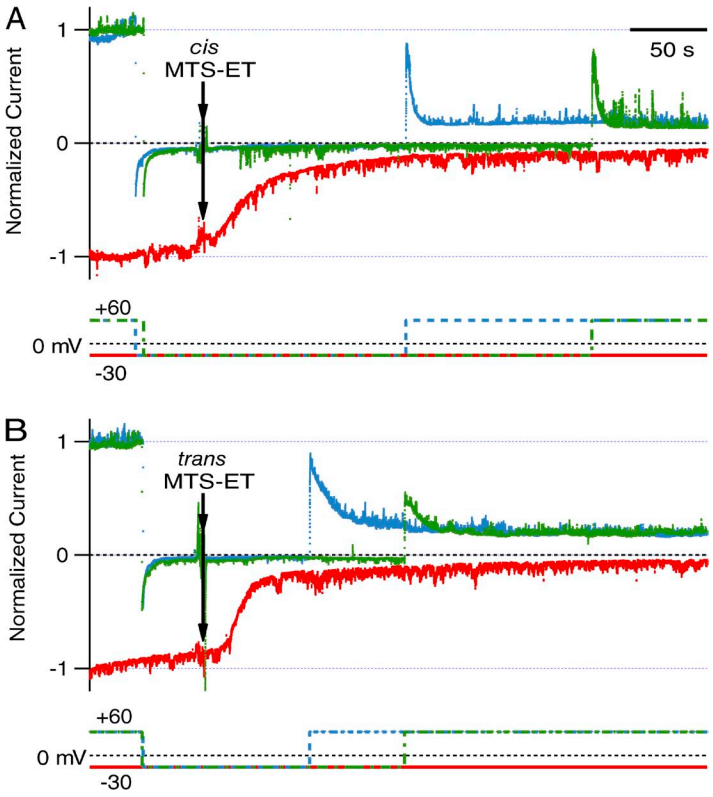

Figure 4. Protection of S312C channels from reaction with MTS-ET by His_6-tag blockade. Records from three experiments are superimposed in each panel; the top traces are normalized current, and the bottom traces are voltage, with all plotted against time (relative to the moment of MTS-ET addition). The protection experiments (blue and green traces) used S312C with an amino-terminal His_6-tag, whereas the unblocked control experiments (red traces) used S312C from which the His_6-tag had been removed by thrombin treatment. About 4–10 min before the start of each record, 8–9 ng S312C was added to the cis compartment, and the channel activity was allowed to stabilize. At the arrow, while holding at −30 mV, 2.6 mg MTS-ET was added to the cis (A) or trans (B) compartment. In the unblocked control experiments (red traces), reaction with MTS-ET at −30 mV caused a decrease in conductance that was largely complete within 1–2 min. In the His_6-tag protection experiments (blue and green traces), the potential was held at −30 mV for 1–4 min of exposure to MTS-ET. Upon switching to 60 mV, there was a rapid increase in current, representing unblocking of the channels by the His_6-tag, followed by a slower decay of the current, representing reaction with MTS-ET. (No such decay was seen without MTS addition.) The relatively large peak currents after unblocking show that His_6-tag blockade protected Cys-312 from reaction. Note that the reaction rate of cis MTS-ET with S312C channels is voltage dependent (see Fig. 6 B); the relevant rate here is that at −30 mV (seen in the unblocked control experiment), rather than the faster rate seen at 60 mV. Solutions were as in Fig. 2. Some of the voltage traces are shown as dashed lines so that all the superimposed traces can be seen. The time scale bar applies to both panels.

experiments with mutant T-domain S312C that demonstrated protection from reaction with both cis and trans MTS-ET (Fig. 4). In brief, Fig. 4 shows that after a period of MTS-ET exposure sufficient for complete reaction of channels without a His_6-tag (red traces), channels blocked by their amino-terminal His_6-tag at −30 mV remained largely unreacted, but reaction occurred promptly upon unblocking at 60 mV (blue and green traces). In similar experiments, we demonstrated that T301C and M314C mutant channels were protected from reaction with cis MTS-ET, and S305C channels were protected from cis and trans MTS-ACE. We also showed protection of L304C channels from reaction with cis pCMBS; this reagent, whose preference for the ionized thiolate

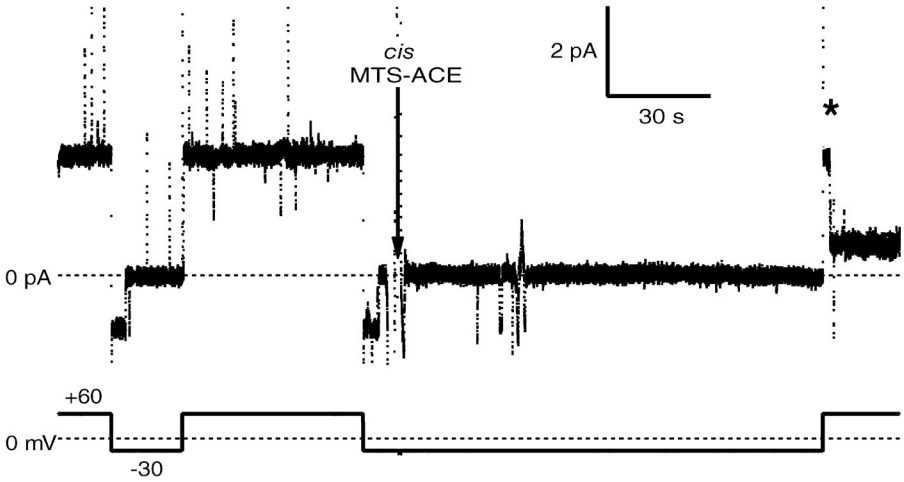

Figure 5. Protection of a single S305C channel from reaction with cis MTS-ACE by His_6-tag blockade. Two additions of S305C totaling 50 ng were made to the cis compartment 7–11 min before the start of the record. After a 45-pS channel opened at 60 mV (3 min before the start of the record), the potential was pulsed between −30 and 60 mV to establish normal His_6-tag blocking and unblocking behavior. After blocking again at −30 mV, 400 μg MTS-ACE was added to the cis compartment (at the arrow), and the potential continued to be held at −30 mV for 2 min of MTS-ACE exposure. (During this period, there were a few brief unblocking events of ∼1 s total duration, but no reaction.) Upon switching back to 60 mV, the conductance increased rapidly to its normal (unreacted) level as the channel unblocked, followed 2 s later by a drop to 10 pS (marked by an asterisk), representing reaction of the channel. Solutions were as in Fig. 2, except that the buffers were 20 mM MES, pH 6.0 (cis), versus 5 mM HEPES, pH 8.0 (trans).

group is not as pronounced as that of MTS reagents (Parikh et al., 2011), was chosen so that we could do the experiments more easily, without raising the cis pH. It was difficult to do a convincing protection experiment with the predominantly trans-exposed L307C and G309C because of the small magnitudes of their macroscopic MTS-ET effects. (For what it is worth, we tested V347C, a position in the TH8–TH9 loop, which responds to trans but not to cis MTS-ET [Huynh et al., 1997], and for which we determined a relatively high reaction rate [$\sim 10^4$ M^{-1} s^{-1}], suggesting that it is well exposed on the trans side. We found that His_6-tag block did not protect V347C channels from reaction with trans MTS-ET.)

If, hypothetically, the His_6-tag plugged only the trans end of the channel, the rest of the channel would be expected to equilibrate with the low pH of the cis solution. Because MTS reacts mainly with the ionized S^- form of the sulfhydryl group (Roberts et al., 1986), His_6-tag block might inhibit cis MTS reaction indirectly by lowering the local pH at the cysteine residue. We investigated this possibility in a series of experiments with S305C channels, starting with a pH gradient of 6.0 (cis) versus 8.0 (trans). In the control experiment, the trans pH was lowered to ~6 after channel formation to mimic the hypothesized effect of His_6-tag block. Under this condition, reaction of 2 mM cis MTS-ACE with unblocked channels at 60 mV was complete within 1 min. In contrast, in the corresponding protection experiments (with the pH 6.0 vs. 8.0 gradient maintained), blocked channels did not react during a 2-min exposure to cis MTS-ACE but reacted within a few seconds upon unblocking; this is shown at the single-channel level in Fig. 5. (As a side note, fast reactions were sometimes observed during brief unblocking events at −30 mV.) Thus, at least in this case, protection from reaction by His_6-tag blocking was not caused by the local pH at the reactive site becoming closer to the cis pH.

Comparison of cis- and trans-side reaction rates in the TH6–TH7 segment

Several of the mutant channels that we have examined reacted with both cis and trans MTS-ET. We wished to compare the reaction rates from the cis and trans sides to quantify the cysteine residue's accessibility to one side or the other (Table 4). For a charged reagent such as MTS-ET, the reaction rates are expected to be voltage dependent; to make a proper comparison, we need to estimate the cis and trans rates at zero voltage. We did this for mutants S305C and S312C by measuring the rates for reaction at several voltages and interpolating to 0 mV (Fig. 6). (For these experiments, we removed the amino-terminal His_6-tag so we could observe the reaction at negative voltages.) At 0 mV, the reaction of MTS-ET with S305C channels was ~2.4 times faster from the cis side than from the trans side (Fig. 6 A). The rate constants had a rather weak, approximately exponential dependence on voltage. For S312C channels, MTS-ET

TABLE 4
Rates of MTS-ET effects on TH6–TH7 segment mutant channels

Mutant	cis pH	mV	k_{cis}	k_{trans}
			M^{-1} s^{-1}	M^{-1} s^{-1}
T300C	7.0	60	40 ± 13 (n = 4)	NE (n = 2)
T301C	6.2	60	15 ± 2 (n = 3)	NE (n = 2)
A302C	5.3	−20	8.1 ± 0.2 (n = 2)	NE (n = 2)
A303C	7.2	40–60	1,094 ± 91 (n = 3)	NE (n = 3)
L304C	6.6	60	68 ± 9 (n = 3)	NE (n = 2)
S305C[a]	5.3	0	192 ± 40	79 ± 10
I306C	5.3	−30 or 30[b]	4.4 ± 0.8 (n = 2)	5.6 ± 0.2 (n = 2)
L307C	5.3	30–40	33 ± 9 (n = 3)	607 ± 377 (n = 6)
G309C	5.3	20–60	40 ± 19 (n = 4)	750 ± 479 (n = 4)
I310C[c]	6.3	60	44 (n = 4)	<2 (n = 3)
S312C[a]	5.3	0	7.4 ± 1	11.4 ± 2
V313C	6.3	20–60	8 ± 4 (n = 4)	NE (n = 2)
M314C	6.3	20–60	10 ± 4 (n = 6)	NE (n = 4)
G315C[c]	5.2	30–60	7 (n = 6)	<0.5 (n = 4)
I316C	5.2	40	32 ± 10 (n = 3)	NE (n = 2)
A317C	7.0	60	113 ± 72 (n = 3)	NE (n = 2)

The rates are given as mean ± SD, with n being the number of macroscopic experiments, except where indicated otherwise. The trans pH was 7.2 for all experiments. The His_6-tag was removed from the T-domain for the experiments with A302C, S305C, I306C, and S312C. NE, no effect.
[a]The rates for S305C and S312C are from the fitted lines in the graphs in Fig. 6. The error range was estimated by eye.
[b]For I306C, k_{cis} was measured at 30 mV and k_{trans} was measured at −30 mV.
[c]A trans MTS-ET effect was observed in single-channel experiments with I310C and G315C, but it was too slow to be detected in macroscopic experiments. The rates given here were estimated from the single-channel waiting times. In some of the experiments with trans MTS-ET, the channel did not react after a long waiting time, so the value given for the rate is an upper limit. Here, n is the number of reaction events.

reaction at 0 mV was ~1.5 times faster from the trans side than from the cis side (Fig. 6 B). For this mutant, the voltage dependence of the cis MTS-ET reaction rate was about twice as steep as that seen for S305C, whereas the reaction rate of trans MTS-ET was essentially independent of voltage. Although a quantitative analysis of the voltage dependence of the reaction rates is beyond the scope of this paper, we note that the voltage dependence of MTS-ET reaction with S312C channels was steeper from the cis side and weaker from the trans side, as compared with that of S305C channels, consistent with a location closer to the trans side.

For L307C channels, we could make a rough estimate of cis- versus trans-side accessibility from experiments at positive voltage. As shown in Fig. 7, the reaction at 30 mV with trans MTS-ET (red trace) was ~10 times faster than that with cis MTS-ET (cyan trace). The effect of the positive voltage should be to drive the positively charged MTS-ET into the channel from the cis side and to drive it out on the trans side. Thus, extrapolating to 0 mV, we would expect that the ratio of trans to cis rates would be even more extreme.

We also measured reaction rates of uncharged MTS reagents, which are not susceptible to the effects of voltage described above. Because of the lower reactivity of these reagents, as compared with MTS-ET, the possibility of slow washout effects is a greater problem in macroscopic experiments; hence, we present only results from single-channel experiments, in which the reaction of a channel in the membrane is more readily distinguished from a washout effect (Table 2).

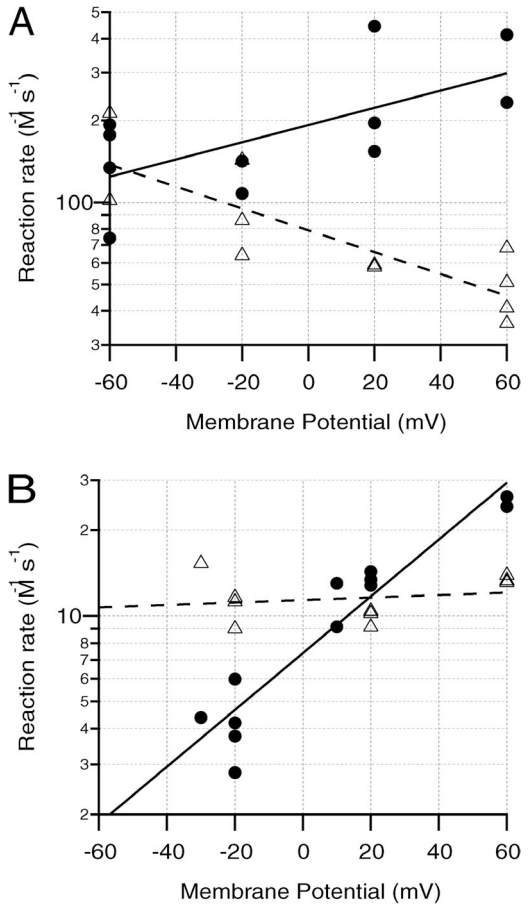

Figure 6. Estimation of MTS-ET reaction rates at 0 mV. (A) S305C. (B) S312C. Each graph is a semilog plot of the second-order rate constant, k, for cis (●) or trans (△) MTS-ET reaction versus voltage. Each data point represents one experiment. Linear fits of log(k) versus voltage are shown. Interpolating to 0 mV gives $k_{cis}/k_{trans} \approx 2.4$ for S305C and 0.7 for S312C. Solutions were as in Fig. 2, except that for A, the buffers were 30 mM MES, pH 5.3 (cis), versus 50 mM HEPES, pH 7.2 (trans).

Effects of MTS reagents on TH8–TH9 mutant channels

Comparison of cis- and trans-side reaction rates. An earlier study identified channel-lining residues in the TH8–TH9 segment of T-domain (Huynh et al., 1997). We measured cis- and trans-side reaction rates for selected residues in this segment to determine the relative alignment between TH6–TH7 and TH8–TH9. Fig. 8 presents two examples from TH8. Fig. 8 A shows that A334C reacted faster with cis (cyan trace) than with trans (red trace) MTS-ET; from Fig. 8 B we can see that L338C reacted faster with trans than with cis MTS-ET. (In each of these experiments, we used T-domain without a His_6-tag and balanced the effects of voltage on cis- and trans-side

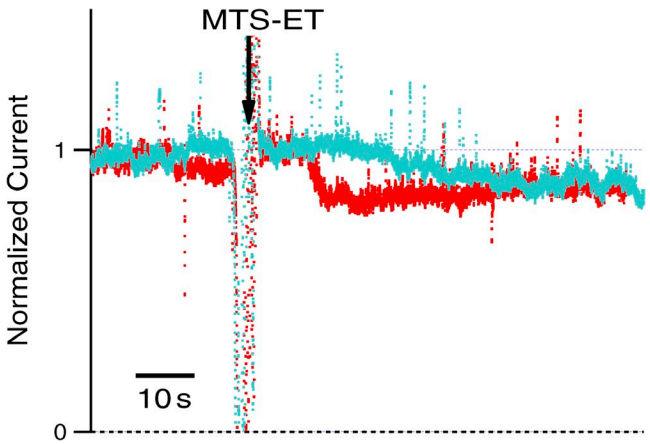

Figure 7. Comparison of cis- and trans-side reaction rates of MTS-ET with T-domain mutant L307C. Records from two experiments are superimposed, showing normalized current versus time. About 7–10 min before the start of the record, 4–8 ng L307C was added to the cis compartment, and the channel activity was allowed to stabilize. At the arrow, 200 μg MTS-ET was added to the cis (cyan trace) or trans (red trace) compartment, resulting in a decrease in current of ~19%. The pseudo-first order rate constants were estimated as $k_{1,cis} = 0.0241\ s^{-1}$ and $k_{1,trans} = 0.247\ s^{-1}$ for the cis- and trans-side experiments, respectively. Solutions were as in Fig. 2. The holding potential was 30 mV. The trans MTS-ET experiment was the same one depicted in Fig. 2. In the cis MTS-ET experiment, there was a further slow decrease in current after the end of the record, presumably because of channel gating or washout (see Data analysis in Materials and methods), but it was disregarded in the analysis.

reaction rates by holding at 30 mV in the cis experiments and −30 mV in the trans experiments, so that the voltage was always driving MTS-ET into the channel. The ratio $k_{cis}(30\ mV)/k_{trans}(-30\ mV)$ is taken as a rough approximation to $k_{cis}(0\ mV)/k_{trans}(0\ mV)$.) These and other results from the TH8–TH9 segment are summarized in Table 5.

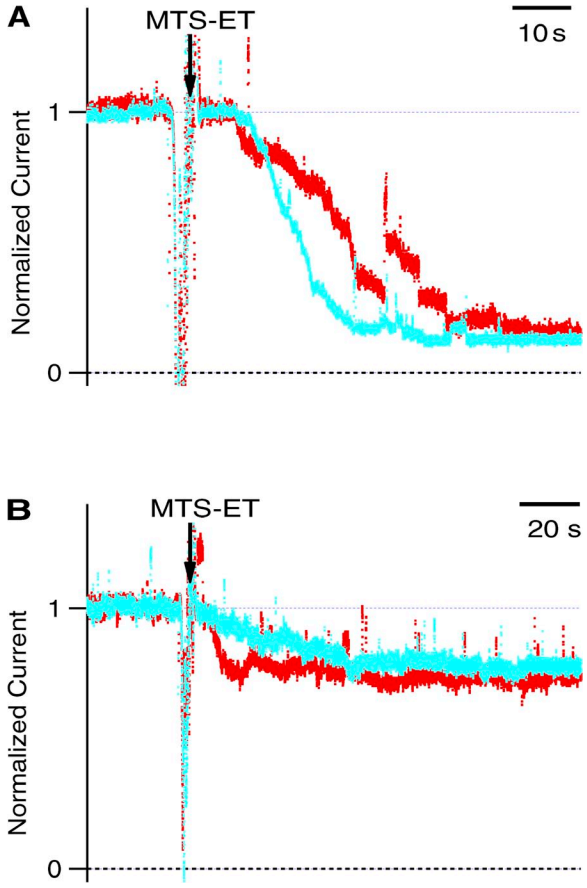

Figure 8. Comparison of cis- and trans-side reaction rates of MTS-ET with T-domain TH8 segment mutants A334C and L338C. Records from two experiments are superimposed in each panel, showing normalized current versus time. (Both negative and positive initial currents were normalized to +1.) T-domain with the His_6-tag removed was used in all four experiments. (A) Multiple additions of A334C totaling 0.1–1 ng were made to the cis compartment 7–18 min before the start of the record, and the channel activity was allowed to stabilize. While holding, respectively, at 30 or −30 mV, 200 µg MTS-ET was added (at the arrow) to the cis or trans compartment (cyan or red trace), causing a conductance decrease of 87 or 85%. Using the 85% value in both cases, Eq. 1a gives $k_{1,cis} = 0.107\ s^{-1}$ and $k_{1,trans} = 0.0297\ s^{-1}$. (The erratic jumps in current occurred frequently for this mutant after MTS-ET addition.) (B) 1–8 ng L338C was added to the cis compartment 8–9 min before the start of the record. While holding, respectively, at 30 or −30 mV, 200 µg MTS-ET was added (at the arrow) to the cis or trans compartment (cyan or red trace), causing a conductance decrease of ∼21 or 23%. (For the cis MTS-ET experiment, 21% was the amount of the fast component of the decrease; there was also a slower component extending ∼25 min beyond the end of the record.) Using the 23% value in both cases, Eq. 1a gives $k_{1,cis} = 0.0235\ s^{-1}$ and $k_{1,trans} = 0.179\ s^{-1}$. For both panels, solutions were as in Fig. 2.

Determining the conductance state in which reaction occurs. For selected mutants in the TH8 segment, we observed the effect of trans MTS-EA on single channels, using 1,000-Hz filtering as we described above for TH6–TH7 segment mutants. We found that for both A334C and L338C channels, reactions occurred primarily in the open state, rather than in the flicker-closed state (Table 3).

DISCUSSION

We have examined a series of cysteine mutations in segment TH6–TH7 of the DT T-domain to ascertain the locations of the cysteine residues in the open-channel state of the protein. In particular, we hoped to learn which residues line the channel and to estimate their relative accessibility to the cis and trans solutions. We also examined mutations in the TH8–TH9 segment so that we could try to determine the alignment between the TH6–TH7 and TH8–TH9 segments.

Identification of channel-lining residues in segment TH6–TH7

We applied SCAM (Karlin and Akabas, 1998) to residues 300–317 of the T-domain, an uncharged segment that roughly corresponds to TH6–TH7 (Fig. 1, inset). We found that all of the tested channels showed an effect of MTS-ET, MTS-ACE, or MTS-glucose (Tables 1 and 2). (G311C was not included because of its noisy conductance.) 10 of the mutants showed a decrease in single-channel conductance in response to MTS reaction: T301C, A302C, S305C, I306C, L307C, P308C, G309C, S312C, M314C, and G315C (Tables 1 and 2). MTS reaction with T300C, A303C, L304C, V313C, I316C, and A317C channels caused a total loss of conductance that most likely represented channel closure, although a nearly complete decrease in single-channel conductance is also a possibility. I310C channels showed an increase in flickering upon MTS reaction but no change in single-channel conductance. We note that G315C showed an abnormally high single-channel conductance (about twice that of WT), so it may not be representative of the native channel structure.

Mapping of transmembrane topography: Overview

One can estimate the position of a cysteine residue in the channel by comparing the rate constants, k_{cis} and k_{trans}, for reagent added to the cis or trans solution, respectively (Wilson and Karlin, 1998; Karlin, 2001). This method of analysis eliminates local factors such as the reactivity of the cysteine, allowing us to focus on the difference in accessibility to the site from the two sides. For convenience, we define a relative accessibility value,

$$f \equiv 1/(1 + k_{cis}/k_{trans}). \quad (3)$$

This value can range from f = 0 for a cysteine that is accessible only to cis reagent to f = 1 for a cysteine that is accessible only to trans reagent. In the simplest diffusion model for an uncharged reagent in a channel of uniform diameter, f equals the fractional distance of the reactive site from the cis interface, relative to the total channel length. As we shall see, the T-domain channel probably does not have a uniform diameter, but we think that f is still useful for comparing the relative positions of different cysteine residues.

Mapping of the TH6–TH7 segment

The pattern of reactive residues in the TH6–TH7 segment gives no clear sign of the periodicity characteristic of an α helix (3.6 residues) or a β sheet (two residues) with one side exposed to the channel lumen. The pattern of accessibility to cis- and trans-side MTS reagents does, however, show a trend, from cis-side only (residues 302–304) to trans-exposed (residues 305–312), and back to cis-side only (residues 313–314) (Table 1). This suggests that the TH6–TH7 segment may assume some kind of hairpin structure within the channel. We wished to extend this analysis to residues that react from both sides by comparing the reaction rates of cis and trans MTS compounds.

We plotted the relative accessibility value, f, for 16 residues in the TH6–TH7 segment (Fig. 9 A). Our initial suspicion that TH6–TH7 forms a hairpin-like structure is supported by these more quantitative results. (This picture is also generally consistent with the slower MTS reactions observed for more cis-exposed residues, when the cis pH is low.) A remarkable feature of the data is the near absence of intermediate values of f. Aside from S305C and S312C (and I306C with MTS-ET), all the residues examined have f values very close to either 0 or 1, even among those residues that are accessible to both cis and trans MTS reagents. Accessibility changes very abruptly, from cis-exposed residue 304 to mostly trans-exposed residue 307, and from mostly trans-exposed residue 309 to cis-exposed residue 314. (For the moment, we neglect residue 310; taking it into account would make the changes even more abrupt.) It seems clear that these short stretches of polypeptide chain are not long enough to span the full thickness of a lipid bilayer.

The simplest solution is to suppose that TH6–TH7 forms a constriction occupying a relatively small portion of the channel length. If this constriction hinders the diffusion of the reagent, then f would essentially measure progress through the constriction rather than through the whole channel. Although we do not have a detailed model for the structure of the TH6–TH7 segment in the channel, it is instructive to map our results onto the aqueous crystal structure (Fig. 9 B). We find a substantial (albeit imperfect) correlation between our calculated f values and the vertical direction in the figure. This suggests that the TH6–TH7 segment in the open channel might form such an open hairpin structure, oriented with the Pro-308 ring pointing toward the trans side.

Taking the proposed channel constriction to an extreme limit, one might ask if it could completely block the passage of the MTS reagent through the channel. We think that this is not the case, as our largest reagent, MTS-glucose, reacted from either side at several positions in the TH6–TH7 (305, 307, and 312; Table 2) and TH8–TH9 (331 and 359; Table 5) segments.

Evidence for reaction in the open-channel state

We are trying to determine the location of the TH6–TH7 segment in the open-channel state of the T-domain,

TABLE 5

Magnitude and rates of MTS effects in macroscopic experiments on TH8–TH9 segment mutant channels

Mutant	cis pH	trans pH	MTS reagent	Conductance change (%)	k_{cis}	k_{trans}
					$M^{-1}\,s^{-1}$	$M^{-1}\,s^{-1}$
Q331C	7.0	7.2	ET	−90 ± 5 (n = 4)	45.0 ± 0.4 (n = 2)	12.3 ± 0.8 (n = 2)
"	7.0	8.0	Glucose	−74 ± 8 (n = 4)	13 ± 1 (n = 2)	5 ± 1 (n = 2)
A334C	5.3	7.2	ET	−83 ± 3 (n = 4)	151 ± 20 (n = 3)	44 ± 2 (n = 2)
L338C	5.3	7.2	ET	−25 ± 2 (n = 4)	24 ± 6 (n = 2)[a]	414 ± 212 (n = 4)
A341C	5.3	7.2	ET	−11 ± 2 (n = 4)	7 ± 2 (n = 2)	52 ± 13 (n = 2)
V347C	5.3	7.2	Glucose	−24 ± 4 (n = 6)	11 ± 7 (n = 4)[a]	1,776 ± 629 (n = 3)
Y358C	5.3	7.2	ET	−53 ± 16 (n = 3)	NE (n = 2)	11 ± 7 (n = 4)
N359C	6.0	8.0	Glucose	−61 ± 7 (n = 4)	34 ± 4 (n = 3)	73 ± 9 (n = 3)

The percent conductance change and rates are given as mean ± SD, with n being the number of experiments. Both cis and trans MTS results were used in calculating the conductance change, if they were generally in agreement. The percent conductance change and reaction rate could not always both be determined for a given experiment, so the n values for k_{cis} and k_{trans} do not necessarily add up to the n value given for the conductance change. In the experiments with MTS-ET, k_{cis} and k_{trans} were measured at 30 and −30 mV, respectively. Each of the mutant T-domains had its His_6-tag removed, with the exception of V347C and N359C. NE, no effect.

[a]Cis MTS reagent, even at high concentrations, produced a slow effect on the conductance. It is possible that this was caused by reaction in the cis solution, followed by slow washout of channel activity from the membrane; thus, the value for k_{cis} should be taken as an upper limit.

so we would like to know whether the reactions that we have measured actually occurred in the open state and, indeed, whether the channel has a single open-state structure. It is known that DT and its T-domain undergo several conformational changes upon exposure to a lipid membrane at low pH, from a water-soluble protein (Bennett et al., 1994) to a membrane-inserted channel with its amino-terminal portion translocated across the membrane (Senzel et al., 1998; Oh et al., 1999b). Furthermore, it has been reported that the T-domain and other DT constructs can assume several pretranslocation and translocated conformations that exchange with one another (Rosconi and London, 2002; Rosconi et al., 2004; Zhao and London, 2005; Lai et al., 2008; Wang and London, 2009). The channel states in our study had the amino-terminal end of the T-domain translocated across the membrane, as indicated by His_6-tag blocking at negative voltages (Senzel et al., 1998), so we need not be concerned here with pretranslocation states.

The results obtained previously from a SCAM study of the TH8–TH9 segment of the T-domain suggest that, even after a channel has opened, at least two states are intermingled: the open state and a brief flicker-closed state (Huynh et al., 1997). Despite the low occupancy probability of the flicker-closed state (~5%), reaction in this state is not a negligible possibility. Of the 10 mutant channels with a cysteine residue in the TL5 loop that were examined, about half had the majority of their assigned reactions in the brief flicker-closed state, and all indicated greater reactivity in the flicker-closed state than in the open state (Huynh et al., 1997). Furthermore, the pattern of reactive residues did not suggest any standard secondary structure but might be consistent with a mobile structure (see discussion below).

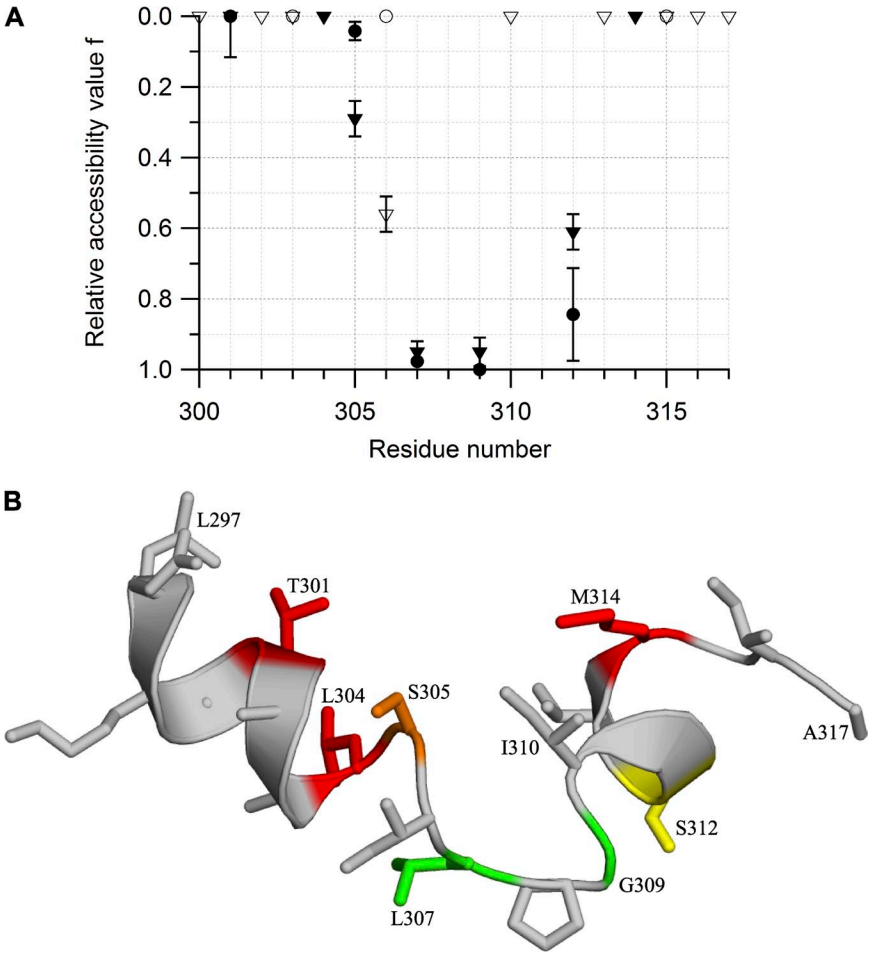

Figure 9. Analysis of results for the TH6–TH7 segment. (A) Plot of the relative accessibility value, f, against residue number for the T-domain TH6–TH7 segment. Based on macroscopic experiments using MTS-ET (▼, ▽) or single-channel experiments using MTS-glucose (●, ○), f was calculated from Eq. 3. Closed symbols are used for residues that were observed to react primarily in the open state, as well as for those that showed protection from reaction by His_6-tag blocking; open symbols are used for the other residues. (Data for G315C are included, despite its abnormally high single-channel conductance.) Note that in the MTS-ET experiments (except with A302C, S305C, I306C, and S312C), the rates were measured at positive voltage, which may exaggerate the proximity of the mutated residues to the cis side. This panel is based on data in Tables 1, 2, and 4. Using a Taylor series approximation for the function $f(x, y) = 1/(1 + x/y)$, we estimated its mean as $\mu_f \approx 1/(1 + \mu_x/\mu_y)$, and its SD as $\sigma_f \approx (\mu_y^2\sigma_x^2 + \mu_x^2\sigma_y^2)^{1/2}/(\mu_x + \mu_y)^2$. For macroscopic data, μ is the mean of k, σ is the SD of k, and the x and y subscripts refer to cis and trans, respectively. For single-channel data, $\mu = \tau$ (the mean waiting time), $\sigma = \tau/n^{1/2}$ (an estimate of the SD of τ, based on the assumption of exponentially distributed waiting times), and the x and y subscripts refer to trans and cis, respectively. The error bars represent the SD of f. Error bars smaller than the symbols were omitted. (B) Mapping of the relative accessibility values, f, for the TH6–TH7 segment onto the aqueous crystal structure of DT. The segment from residues 297–317 is shown. Residues represented by closed symbols in A are colored red, orange, yellow, or green to represent f values of ~0.0, 0.2–0.3, 0.6–0.8, or 1.0, respectively. There is a rough correlation between f and the vertical position in the figure. Residues 297–317 were excerpted from the crystal structure of whole DT (Bennett et al., 1994), available from the Protein Data Bank (Berman et al., 2000) under accession no. 1DDT, and displayed using PyMOL (1.7.2.1). The polypeptide backbone is represented as a ribbon in α-helical regions and as a narrow tube in loop regions. Side chains are shown as stick figures.

We have used two approaches to address the state of reaction: (1) recording single-channel currents with sufficient time resolution to distinguish reaction in the open state from reaction in the flicker-closed state, much as done by Huynh et al. (1997); and (2) showing that the reagent accessed the cysteine residue through the channel.

Using the first approach, for all the mutants that we examined in the TH6–TH7 segment (T301C, S305C, L307C, G309C, and S312C) and TH8 segment (A334C and L338C), using 1,000-Hz filtering, most of the reactions appeared to occur in the open state (Table 3). Thus, at the least, there is no positive evidence that reaction in states other than the open state had a major effect on our results. Of course, we cannot rule out the possibility that there might be multiple conformational states with the same single-channel conductance, or that there might be multiple states that interconvert too rapidly for us to resolve, so that the conductance we measured would have been an average of several distinct conductance states.

The second approach allows us to argue that reaction took place within the channel, as opposed, for instance, to the TH6–TH7 segment flipping out of the membrane beyond the cis interface to react. For a mutant that reacted with a membrane-impermeant reagent such as MTS-ET or MTS-glucose from both the cis and trans sides, it might be considered obvious that reaction occurred in the channel, but, unfazed, we did further experiments using blockade by the amino-terminal His_6-tag to protect cysteine residues from reaction. (The possibility of an interaction between cysteine residues in the TH6–TH7 segment and the His_6-tag was suggested by our observation that MTS reaction affected the blocking rate for several of the mutant channels [unpublished data].) It is believed that the channel closure induced by the amino-terminal His_6-tag at negative voltages represents blocking of the T-domain channel (Senzel et al., 1998, 2000; Gordon and Finkelstein, 2001), although a binding site within the channel has not been determined. Of mutants that can react from both cis and trans sides, we demonstrated that His_6-tag blockade protected T301C, S305C (Fig. 5), and S312C (Fig. 4) channels from MTS reaction. Protection was also observed for two mutants that reacted only from the cis side: L304C and M314C. This was particularly informative for L304C, because the effect of cis MTS reaction was to close the channel (or to reduce the open-channel conductance nearly to zero), so it was not possible to observe directly whether reaction occurred in the open state or in the flicker-closed state. Although the His_6-tag protection experiments indicate that reaction occurred within the channel, they do not give ironclad proof that reaction occurred in the open state. It is possible, for instance, that a mutant could react only in the flicker-closed state, and that the flicker-closed state could be accessed from the open state but not from the blocked state. In addition, the positive charges in the His_6-tag might repel MTS-ET (but not MTS-ACE or pCMBS) electrostatically from a distance.

Another indication of reaction within the channel comes from the decrease in cation selectivity of A302C, S305C, S312C, and G315C channels upon reaction with MTS-ET. Although, strictly speaking, this does not tell us where the cysteine residue was at the moment of reaction, it at least suggests that the cysteine was in the channel after reaction.

Because of its apparently anomalous cis-side accessibility (Fig. 9 A), we wanted to determine whether I310C reacts in the open-channel state; however, the methods that we used for other mutants did not provide persuasive evidence for this mutant. Because MTS reaction with I310C caused an increase in channel flickering without a single-channel conductance change, it was not possible to distinguish reaction in the open state from that in the flicker-closed state. We did see some indication of His_6-tag protection from cis MTS-ET reaction with I310C channels (unpublished data), but these experiments were difficult to interpret because of the significant closing rate at −30 mV of I310C channels without a His_6-tag in the control experiments. Despite all this, the fact that I310C channels reacted with both cis and trans MTS-ET (Table 1), although the trans-side effect was quite slow (Table 4), could be taken as sufficient evidence that reaction occurred within the channel, in which case we should take seriously the assignment of a cis-side location in Fig. 9 A. At first glance, this would appear to complicate our topological model for the TH6–TH7 segment, adding an extra jump from trans to cis and one from cis to trans. If the TH6–TH7 segment forms a short constriction in the channel, however, the model in Fig. 9 B automatically offers an explanation for how residue 310, which points up in the figure, could be exposed to the cis side at the same time that residues 309 and 312, which point down, are exposed to the trans side.

The magnitude of the reaction rates

Our approach of comparing cis and trans MTS reaction rates allows us to estimate the relative accessibility of an introduced cysteine residue to one side or the other, without the need to address the multiple factors that could influence the absolute rate. There might be concerns, however, that an unusually low reaction rate could indicate that reaction occurred in a rarely occupied state. We shall address such concerns by comparing the rates that we have measured for T-domain mutants with rates that have been previously determined for other channels. Before this, however, we mention two obvious factors that must be taken into account. First, if a T-domain mutant has its cysteine residue located, for instance, near the cis end of the

channel, and MTS is added to the trans compartment, then the MTS concentration at the reactive site is expected to be much less than the nominal concentration, leading to an underestimate of the second-order rate constant. Thus, the larger of the pair of rate constants (k_{cis} and k_{trans}) should give a better estimate of the true reaction rate. Second, MTS reaction with the ionized thiolate group is much faster ($>5 \times 10^9$ times) than that with the protonated thiol (Roberts et al., 1986), so a higher pH at the reactive site should produce a greater reaction rate. Indeed, for many of the mutant channels (particularly those with an f value near zero; Fig. 9 A), it was clear that raising the cis pH made the MTS reaction faster. In our experiments with a pH gradient (e.g., 5.3 cis vs. 7.2 trans), although we do not know the precise local pH at the reactive site, it is reasonable to suppose that some of the more cis-exposed residues may have experienced a local pH close to 5. Thus, for comparison with published reaction rates obtained near pH 7, it may be appropriate to increase some of our measured rates by up to 100-fold to account for the pH difference.

We now discuss how the rates that we have measured for the reaction of uncharged MTS compounds with T-domain mutant channels compare with published values for somewhat similar channels. The reaction of such compounds with cysteine residues in a channel is often slower than with small thiol molecules in aqueous solution, because of limitations on access to the reactive site, localized steric hindrance, and factors that make ionization of the SH group less likely, such as a negative local electrical potential lowering the local pH, or a lower dielectric constant (Pascual and Karlin, 1998). For instance, the rate constants for reaction of 2-hydroxyethyl MTS (MTS-EH) with cysteine residues in the open acetylcholine receptor (AChR) channel are only 0.25–8 M^{-1} s^{-1}, compared with 9,530 M^{-1} s^{-1} for reaction with 2-mercaptoethanol (Zhang and Karlin, 1997; Pascual and Karlin, 1998). In this context, the rates that we have measured for MTS-ACE and MTS-glucose reaction with TH6–TH7 segment mutants, in the range of 2 to 400 M^{-1} s^{-1} (Table 2), do not seem unusually slow. In fairness, the T-domain channel, given its relatively moderate cation selectivity, probably does not have the extremely negative local potential found near the selectivity filter of the AChR channel; if we restrict our comparison to positions with a positive or small negative local potential, the rate of MTS-EH reaction with the open AChR channel is in the range of 4 to 8 M^{-1} s^{-1} (Pascual and Karlin, 1998), still comparable to our values for TH6–TH7 mutant channels. Another example illustrating the effect of a negative local potential is given by the colicin E1 channel, in which the reaction rate of the native Cys-505 with methyl MTS (k of $\sim$5 M^{-1} s^{-1} at symmetric pH 7.2) increased more than 10-fold when negatively charged Asp-473 (presumed to be nearby) was mutated to neutral Asn (Kienker et al., 2008).

Positively charged MTS reagents tend to be more reactive than uncharged reagents, presumably because of their electrostatic interaction with the thiolate anion. For instance, MTS-EA and MTS-ET react with 2-mercaptoethanol 15–21 times faster than does methyl MTS (Stauffer and Karlin, 1994) and 8–22 times faster than does MTS-EH (Pascual and Karlin, 1998). A negative local electrical potential in the channel has two opposing effects on the reaction rate of a positively charged MTS reagent: both to decrease the rate by lowering the local pH and to increase the rate by increasing the local MTS concentration. Thus, it is not surprising that in the open AChR channel, MTS-EA can react much more rapidly (roughly 8- to 70,000-fold) than MTS-EH, with the rates for MTS-EA in the range of 2 to 17,000 M^{-1} s^{-1} (Zhang and Karlin, 1997; Pascual and Karlin, 1998). Although we have not extensively studied reaction rates for positively charged MTS reagents with T-domain mutants, because of the complicating effect of the membrane potential, the rates for MTS-ET reaction shown in Fig. 6 were in the range of 3 to 500 M^{-1} s^{-1}, comparable to the low end of the results for the AChR channel. Rates for MTS-ET reaction with TH8–TH9 segment mutants were in the same range (Table 5), except for V347C, which, as mentioned earlier, reacts with trans MTS-ET with a rate of $\sim 10^4$ M^{-1} s^{-1}.

Mapping of the TH8–TH9 segment

A consequence of the supposition that the TH6–TH7 segment forms a short constriction in the channel is that other channel-lining segments at the level of the constriction should also show an abrupt change in f with distance. We examined the TH8–TH9 segment to see if this was true.

Knowledge of the structure of the TH8 segment would aid in the interpretation of our results. It has long been believed that the TH8–TH9 segment inserts into the membrane as an α-helical hairpin that contributes to the channel lining (Choe et al., 1992). Site-directed spin-labeling studies indicated that TH8 and TH9 form transmembrane α helices (Oh et al., 1996, 1999a). Based on the relative accessibility of polar and nonpolar paramagnetic reagents to the spin label, as well as on the mobility of the spin label, it was concluded that TH8 and the TL5 loop (between TH8 and TH9) lie at a lipid–protein interface (with TL5 also forming an α helix) and TH9 lies at a lipid–water interface. A SCAM study found that residues in TH8 and the TL5 loop (but almost none in TH9) showed effects of reaction with MTS compounds, suggesting that they line the channel; however, the pattern of reactivity did not suggest a secondary structure (Huynh et al., 1997). The stretches of reactive residues in TH8 (11 of the residues from 329–341) and the TL5 loop (12 of the residues from 347–359) correspond roughly to the TH8 transmembrane segment (328–343)

and TL5 helical segment (347–355, or perhaps beyond) identified using the spin labels.

After years of rumination, we have begun to see hints of helical structure in the data of Huynh et al. (1997). Fig. 10 A is a helical-wheel diagram coded to show the effect of the positively charged reagent MTS-EA on a series of mutant T-domain channels with single-cysteine substitutions at residues 329–341, the reactive stretch in TH8. Placing a positively charged group within this cation-selective channel is expected to decrease the single-channel conductance, whether electrostatic or steric effects dominate. Mutants for which MTS-EA reaction caused an anomalous increase in single-channel conductance, together with an increase in flickering, are clustered on one face of the putative α helix (residues labeled with a black background); this is the lipid-exposed face identified in spin-label studies (Zhan et al., 1995; Oh et al., 1999a). (The effects of MTS-EA reaction in TL5 [Huynh et al., 1997] likewise suggest a helical structure that matches the spin-label results, but the pattern is less pronounced.) Our working hypothesis is that the reactive segments in TH8 and TL5 are α helical, with one face of each helix normally lining the channel and the opposite face exposed to lipid. MTS reacts primarily with the ionized S^- form of the sulfhydryl group, but the protonated SH form is expected to predominate in a low dielectric lipid-facing environment. We must therefore suppose that the helices are mobile, so that the face that normally contacts lipid is transiently exposed to an aqueous environment. Our results indicate that residues on the left face of the helix in Fig. 10 A (334 and 338) react primarily in the open state (Table 3), so we might imagine that residues on the right face react in the flicker-closed state. It is not surprising that attaching a positively charged group to a lipid-facing surface of the protein would have strange effects on the channel, such as increasing the conductance and flickering, perhaps indicating a perturbation of the channel structure.

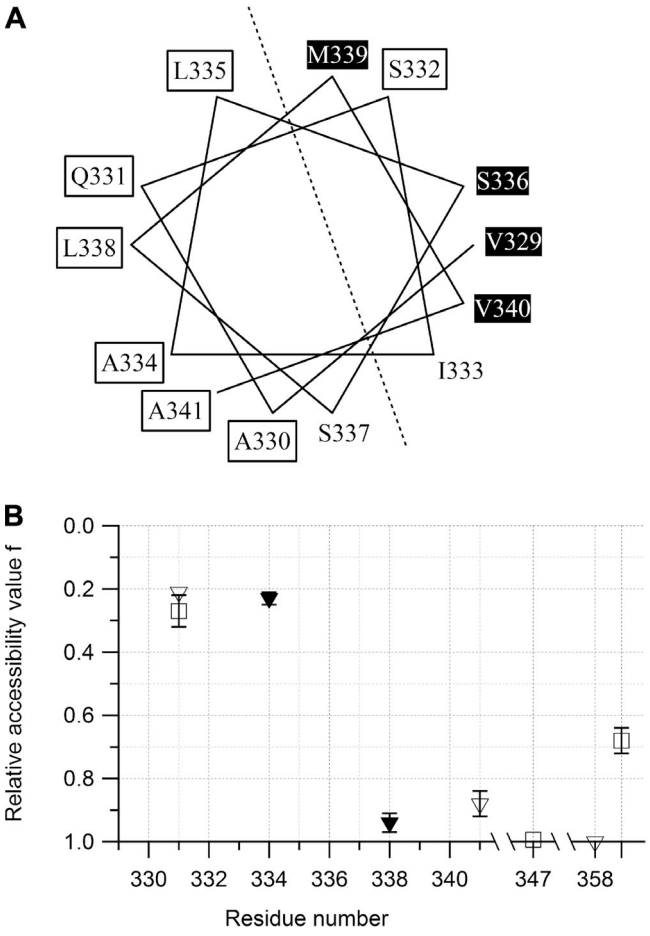

Figure 10. Analysis of results for the TH8–TH9 segment. (A) Helical-wheel diagram based on the results of Huynh et al. (1997) for T-domain segment TH8. The effect of MTS-EA on single-cysteine mutants is indicated. Plain boxed labels, positions at which MTS-EA reaction caused a decrease in single-channel conductance; boxed labels with a black background, positions at which MTS-EA reaction caused an increase in single-channel conductance and an increase in flickering; plain labels, no effect of MTS-EA. The dashed line, based on spin-label studies, divides lipid-exposed residues (right side) from protein-exposed residues (left side) (Zhan et al., 1995; Oh et al., 1999a). (B) Plot of the relative accessibility value, f, against residue number for the T-domain TH8–TH9 segment. Based on macroscopic experiments using MTS-ET (▼, ▽) or MTS-glucose (□), f was calculated as in Fig. 9. Also as in Fig. 9, closed symbols are used for residues that were observed to react primarily in the open state; open symbols are used for the other residues. The sign of the voltage in the MTS-ET experiments was such as to promote MTS-ET entry into the channel. This panel is based on data in Table 5. The error bars represent the SD of f.

Can we reconcile this view with the spin-label results? Whereas the spin-label studies place TH8 and TL5 at a lipid–protein interface, in our picture they are at a lipid–water interface lining the channel. One possibility, of course, is that different membrane-inserted states of the T-domain were detected by the SCAM and spin-label studies. Alternatively, perhaps the indications that the spin label was facing a protein environment (low mobility and low accessibility to paramagnetic reagents) are consistent with a confined aqueous channel environment (Gross et al., 1999). The lack of observed reactions in TH9 is another puzzle, given the spin-label results (Oh et al., 1996), as well as the effects on channel conductance and pH dependence of mutations at residue E362 (Mindell et al., 1994). We suppose that residues in TH9 may be inaccessible to MTS reagents for steric reasons.

In this work, we did not examine the presumed lipid-facing residues in TH8, focusing instead on the residues that we think truly line the aqueous channel. Fig. 10 B shows f values calculated from the data in Table 5 at several positions in the TH8–TH9 segment. Similar to our results with TH6–TH7, there is an abrupt transition, from mostly cis-exposed A334C to mostly trans-exposed L338C. This is consistent with these two residues of the TH8 segment lying on opposite sides of the constriction formed (at least in part) by the TH6–TH7

segment. If TH8 is indeed an α helix, then this would represent about one turn of the helix, or a distance of 6 Å along the helical axis. Based on these results, we can construct a model showing the alignment between the TH6–TH7 and TH8 segments (Fig. 11). In the future, we would like to see if a similarly abrupt transition in f occurs in the TH5 transmembrane segment.

Implications of possible alternative structures

In our mapping of the locations of residues in the TH6–TH7 and TH8–TH9 segments, we have tried to use only data for reaction in a well-defined open state of the T-domain channel. Despite these efforts, however, it is possible that the open-channel conductance state is composed of numerous interconverting conformational states that we cannot resolve with our recordings. Here, we briefly consider some possible types of protein motion and their effect on our structural model. (a) A segment could rotate about a membrane-normal axis. We suspect that TH8 may undergo such a motion. The position of each residue along the channel axis would not change, so the relative accessibility from the cis and trans sides would be unaffected by the rotation. (b) A segment could oscillate parallel to the membrane normal. If such oscillations were large enough in amplitude, then all residues should be accessible to reaction from both cis and trans sides, which is not the case for the TH6–TH7 segment. It is hard to rigorously rule out the possibility of smaller-amplitude oscillations, which could produce quantitative inaccuracies in the relative accessibility values that we have calculated. (c) The TH6–TH7 segment could be on the cis side in the open state but move to block the channel in the flicker-closed state. Such a mechanism was suggested by the results of Zhao and London (2005) and Lai et al. (2008). This seems to be inconsistent with our single-channel experiments showing reaction in the open state, combined with our His_6-tag protection experiments, which indicate that reaction occurs within the channel.

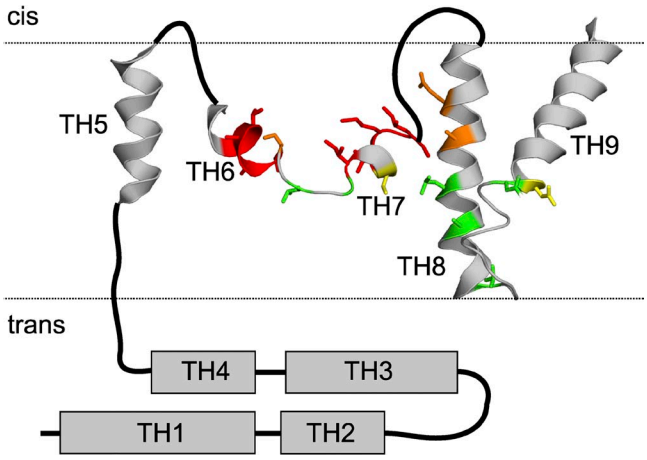

Figure 11. Schematic model of the T-domain in the open-channel state, showing the approximate vertical alignment between the TH6–TH7 and TH8–TH9 segments. As in Fig. 9 B, residues colored red, orange, yellow, and green have f values of ~0.0, 0.2–0.3, 0.6–0.8, and 1.0, respectively. In contrast to Fig. 9 B, here all side chains whose f value was determined are displayed as color-coded stick figures, regardless of whether the state of reaction was determined. (I306C was omitted because of the difference in f values for MTS-ET and MTS-glucose.) The position of TH9 relative to TH8 was left the same as in the crystal structure; we do not mean to imply that it is located away from the pore. Outside of the TH6–TH7 segment, the overall topology is based on the model of Senzel et al. (2000). Residues 275–288, 297–317, and 326–376 (which roughly correspond to segments TH5, TH6–TH7, and TH8–TH9, respectively) were excerpted from the crystal structure (references in the Fig. 9 B legend), reoriented as needed, and displayed using PyMOL. Solid black curves represent loops that connect the segments. The pair of horizontal dotted lines indicates the approximate boundaries of the membrane hydrocarbon region.

Comparison with previous results

Our model for the conformation of the TH6–TH7 segment in the T-domain channel is similar in some respects to previous models. For instance, one model of the so-called "deeply inserted" state of the T-domain, based on spectroscopic methods, places the TH6–TH7 segment within the membrane, nearer the cis side, with both ends of the segment exposed on the cis side, and the amino-terminal end of TH5 on the trans side (Fig. 9 E of Rosconi and London, 2002). A similar conformation for the TH6–TH7 segment was also proposed for a pretranslocation state with the amino-terminal end of TH5 near the cis side, both for the T-domain (Rosconi et al., 2004; Zhao and London, 2005; Lai et al., 2008) and for a construct containing the catalytic domain linked to the T-domain (Wang and London, 2009). There is also evidence that the latter construct can occasionally assume a pretranslocation conformation with the TH5–TH6 loop exposed to the trans side (Wang and London, 2009), reminiscent of the original "double dagger" model for DT (Choe et al., 1992).

Interestingly, mutation of Leu-307 to Arg disrupts the deep insertion of the TH7 segment but still allows the insertion of TH8–TH9 and TH5 (Zhao and London, 2005; Lai et al., 2008). Furthermore, the mutation does not inhibit pore formation but may even enhance the conductance, leading the authors to describe the TH6–TH7 segment as a "cork" that partially blocks the pore. However, the assay used to assess pore formation (based on biocytin entering lipid vesicles to bind to fluorescently labeled streptavidin) does not allow for a distinction between an increased single-channel conductance and an increased number of open channels. Our experiments with this mutant in planar bilayers indicated that its single-channel conductance was comparable to that of L307C channels reacted with MTS-ET and considerably smaller than that of WT T-domain channels (unpublished data). (Note that we have not determined whether insertion of the TH6–TH7 segment was impaired in our

experiments with the L307R mutant.) With P308C, however, reaction with trans MTS-ET did lead to the formation of larger-conductance channels (Table 1, footnote g); perhaps this might reflect the expulsion of the TH6–TH7 segment from the channel.

The role of the TH6–TH7 segment in the translocation of the catalytic domain is unclear. Lai et al. (2008) suggested, based on the segment's hydrophobicity, that it may act as an analogue to the partly unfolded catalytic domain. That is, in the pretranslocation state, the segment may occupy a site in the pore that will serve as a chaperone for the translocating domain, but during translocation it moves out of the way. If this does occur, our results suggest that the TH6–TH7 segment may return in the posttranslocation state to a location similar to that found by Lai et al. (2008) for the pretranslocation state.

Speculations on the channel structure

As noted in the Introduction, it is difficult to construct a model for a monomeric T-domain channel with a large diameter and only TH5, TH8, and TH9 as transmembrane α-helical segments. We now have found that MTS reaction with introduced cysteines at most of the positions from residue 301 to 315 (10 of the 15) causes a single-channel conductance change. From this we can conclude that the TH6–TH7 segment is exposed in the channel lumen, with TH6 and TH7 perhaps remaining α helical as in the aqueous structure (e.g., Fig. 9 B). Because we do not understand how only three helices could make a large channel, increasing their number to five should be helpful, but there is still a problem. Our data indicate that the TH6–TH7 segment occupies only a small part of the channel length, so there are still only three helices available to line the rest of the channel. Is there any precedent for such a structure?

The closest analogue that we are aware of is the recent crystal structure of the ATP-bound $P2X_4$ receptor (Hattori and Gouaux, 2012). It forms a homotrimeric channel with a minimum diameter of ∼7 Å. Although each subunit contributes two α-helical transmembrane segments, it appears that the pore is lined primarily by one helix per subunit, for a total of three. Remarkably, there are sizable gaps between the subunits, which are presumably filled by lipid in the membrane environment. The transmembrane segments are held in place by their interactions with the extracellular domain. It is tempting to speculate that the T-domain channel likewise is lined by three transmembrane helices, TH5, TH8, and TH9, with lipid-filled gaps between the protein segments. The TH6–TH7 segment could reach across the pore, acting as a strut to hold the other segments in place.

We thank Drs. Myles Akabas, Thaddeus Bargiello, Karen Jakes, Charles Peskin, and Russell Thomson for their helpful comments on an early version of the manuscript.

This work was supported by National Institutes of Health grant GM29210.

The authors declare no competing financial interests.

Merritt C. Maduke served as editor.

Submitted: 11 November 2014
Accepted: 9 December 2014

REFERENCES

Bennett, M.J., S. Choe, and D. Eisenberg. 1994. Refined structure of dimeric diphtheria toxin at 2.0 Å resolution. *Protein Sci.* 3:1444–1463. http://dx.doi.org/10.1002/pro.5560030911

Berman, H.M., J. Westbrook, Z. Feng, G. Gilliland, T.N. Bhat, H. Weissig, I.N. Shindyalov, and P.E. Bourne. 2000. The Protein Data Bank. *Nucleic Acids Res.* 28:235–242. http://dx.doi.org/10.1093/nar/28.1.235

Choe, S., M.J. Bennett, G. Fujii, P.M.G. Curmi, K.A. Kantardjieff, R.J. Collier, and D. Eisenberg. 1992. The crystal structure of diphtheria toxin. *Nature.* 357:216–222. http://dx.doi.org/10.1038/357216a0

Donovan, J.J., M.I. Simon, R.K. Draper, and M. Montal. 1981. Diphtheria toxin forms transmembrane channels in planar lipid bilayers. *Proc. Natl. Acad. Sci. USA.* 78:172–176. http://dx.doi.org/10.1073/pnas.78.1.172

Gordon, M., and A. Finkelstein. 2001. The number of subunits comprising the channel formed by the T domain of diphtheria toxin. *J. Gen. Physiol.* 118:471–480. http://dx.doi.org/10.1085/jgp.118.5.471

Greenfield, L., M.J. Bjorn, G. Horn, D. Fong, G.A. Buck, R.J. Collier, and D.A. Kaplan. 1983. Nucleotide sequence of the structural gene for diphtheria toxin carried by corynebacteriophage β. *Proc. Natl. Acad. Sci. USA.* 80:6853–6857. http://dx.doi.org/10.1073/pnas.80.22.6853

Gross, A., L. Columbus, K. Hideg, C. Altenbach, and W.L. Hubbell. 1999. Structure of the KcsA potassium channel from *Streptomyces lividans*: A site-directed spin labeling study of the second transmembrane segment. *Biochemistry.* 38:10324–10335. http://dx.doi.org/10.1021/bi990856k

Hattori, M., and E. Gouaux. 2012. Molecular mechanism of ATP binding and ion channel activation in P2X receptors. *Nature.* 485:207–212. http://dx.doi.org/10.1038/nature11010

Hoch, D.H., M. Romero-Mira, B.E. Ehrlich, A. Finkelstein, B.R. DasGupta, and L.L. Simpson. 1985. Channels formed by botulinum, tetanus, and diphtheria toxins in planar lipid bilayers: relevance to translocation of proteins across membranes. *Proc. Natl. Acad. Sci. USA.* 82:1692–1696. http://dx.doi.org/10.1073/pnas.82.6.1692

Huynh, P.D., C. Cui, H. Zhan, K.J. Oh, R.J. Collier, and A. Finkelstein. 1997. Probing the structure of the diphtheria toxin channel. Reactivity in planar lipid bilayer membranes of cysteine-substituted mutant channels with methanethiosulfonate derivatives. *J. Gen. Physiol.* 110:229–242. http://dx.doi.org/10.1085/jgp.110.3.229

Johnson, N.L., S. Kotz, and N. Balakrishnan. 1994. Continuous Univariate Distributions. Vol. 1. Second edition. John Wiley & Sons, Inc., New York. 756 pp.

Kagan, B.L., A. Finkelstein, and M. Colombini. 1981. Diphtheria toxin fragment forms large pores in phospholipid bilayer membranes. *Proc. Natl. Acad. Sci. USA.* 78:4950–4954. http://dx.doi.org/10.1073/pnas.78.8.4950

Karlin, A. 2001. SCAM feels the pinch. *J. Gen. Physiol.* 117:235–237. http://dx.doi.org/10.1085/jgp.117.3.235

Karlin, A., and M.H. Akabas. 1998. Substituted-cysteine accessibility method. *Methods Enzymol.* 293:123–145. http://dx.doi.org/10.1016/S0076-6879(98)93011-7

Kienker, P.K., K.S. Jakes, and A. Finkelstein. 2000. Protein translocation across planar bilayers by the colicin Ia channel-forming domain: Where will it end? *J. Gen. Physiol.* 116:587–597. http://dx.doi.org/10.1085/jgp.116.4.587

Kienker, P.K., K.S. Jakes, and A. Finkelstein. 2008. Identification of channel-lining amino acid residues in the hydrophobic segment of colicin Ia. *J. Gen. Physiol.* 132:693–707. http://dx.doi.org/10.1085/jgp.200810042

Lai, B., G. Zhao, and E. London. 2008. Behavior of the deeply inserted helices in diphtheria toxin T domain: Helices 5, 8, and 9 interact strongly and promote pore formation, while helices 6/7 limit pore formation. *Biochemistry.* 47:4565–4574. http://dx.doi.org/10.1021/bi7025134

Mindell, J.A. 1993. Mapping the Membrane Topography of the Diphtheria Toxin Channel: A Study in Molecular Cartography. PhD thesis. Albert Einstein College of Medicine, Bronx, NY. 125 pp.

Mindell, J.A., J.A. Silverman, R.J. Collier, and A. Finkelstein. 1994. Structure-function relationships in diphtheria toxin channels: III. Residues which affect the *cis* pH dependence of channel conductance. *J. Membr. Biol.* 137:45–57.

Montal, M. 1974. Formation of bimolecular membranes from lipid monolayers. *Methods Enzymol.* 32:545–554. http://dx.doi.org/10.1016/0076-6879(74)32053-8

Murphy, J.R. 2011. Mechanism of diphtheria toxin catalytic domain delivery to the eukaryotic cell cytosol and the cellular factors that directly participate in the process. *Toxins (Basel).* 3:294–308. http://dx.doi.org/10.3390/toxins3030294

Oh, K.J., H. Zhan, C. Cui, K. Hideg, R.J. Collier, and W.L. Hubbell. 1996. Organization of diphtheria toxin T domain in bilayers: A site-directed spin labeling study. *Science.* 273:810–812. http://dx.doi.org/10.1126/science.273.5276.810

Oh, K.J., H. Zhan, C. Cui, C. Altenbach, W.L. Hubbell, and R.J. Collier. 1999a. Conformation of the diphtheria toxin T domain in membranes: A site-directed spin-labeling study of the TH8 helix and TL5 loop. *Biochemistry.* 38:10336–10343. http://dx.doi.org/10.1021/bi990520a

Oh, K.J., L. Senzel, R.J. Collier, and A. Finkelstein. 1999b. Translocation of the catalytic domain of diphtheria toxin across planar phospholipid bilayers by its own T domain. *Proc. Natl. Acad. Sci. USA.* 96:8467–8470. http://dx.doi.org/10.1073/pnas.96.15.8467

Parikh, R.B., M. Bali, and M.H. Akabas. 2011. Structure of the M2 transmembrane segment of GLIC, a prokaryotic Cys loop receptor homologue from *Gloeobacter violaceus*, probed by substituted cysteine accessibility. *J. Biol. Chem.* 286:14098–14109. http://dx.doi.org/10.1074/jbc.M111.221895

Pascual, J.M., and A. Karlin. 1998. State-dependent accessibility and electrostatic potential in the channel of the acetylcholine receptor. Inferences from rates of reaction of thiosulfonates with substituted cysteines in the M2 segment of the α subunit. *J. Gen. Physiol.* 111:717–739. http://dx.doi.org/10.1085/jgp.111.6.717

Roberts, D.D., S.D. Lewis, D.P. Ballou, S.T. Olson, and J.A. Shafer. 1986. Reactivity of small thiolate anions and cysteine-25 in papain toward methyl methanethiosulfonate. *Biochemistry.* 25:5595–5601. http://dx.doi.org/10.1021/bi00367a038

Rosconi, M.P., and E. London. 2002. Topography of helices 5-7 in membrane-inserted diphtheria toxin T domain: Identification and insertion boundaries of two hydrophobic sequences that do not form a stable transmembrane hairpin. *J. Biol. Chem.* 277:16517–16527. http://dx.doi.org/10.1074/jbc.M200442200

Rosconi, M.P., G. Zhao, and E. London. 2004. Analyzing topography of membrane-inserted diphtheria toxin T domain using BODIPY-streptavidin: At low pH, helices 8 and 9 form a transmembrane hairpin but helices 5-7 form stable nonclassical inserted segments on the cis side of the bilayer. *Biochemistry.* 43:9127–9139. http://dx.doi.org/10.1021/bi049354j

Schraiber, J.G., Y. Mostovoy, T.Y. Hsu, and R.B. Brem. 2013. Inferring evolutionary histories of pathway regulation from transcriptional profiling data. *PLOS Comput. Biol.* 9:e1003255. http://dx.doi.org/10.1371/journal.pcbi.1003255

Senzel, L., P.D. Huynh, K.S. Jakes, R.J. Collier, and A. Finkelstein. 1998. The diphtheria toxin channel-forming T domain translocates its own NH_2-terminal region across planar bilayers. *J. Gen. Physiol.* 112:317–324. http://dx.doi.org/10.1085/jgp.112.3.317

Senzel, L., M. Gordon, R.O. Blaustein, K.J. Oh, R.J. Collier, and A. Finkelstein. 2000. Topography of diphtheria toxin's T domain in the open channel state. *J. Gen. Physiol.* 115:421–434. http://dx.doi.org/10.1085/jgp.115.4.421

Silverman, J.A., J.A. Mindell, H. Zhan, A. Finkelstein, and R.J. Collier. 1994. Structure-function relationships in diphtheria toxin channels: I. Determining a minimal channel-forming domain. *J. Membr. Biol.* 137:17–28. http://dx.doi.org/10.1007/BF00234995

Stauffer, D.A., and A. Karlin. 1994. Electrostatic potential of the acetylcholine binding sites in the nicotinic receptor probed by reactions of binding-site cysteines with charged methanethiosulfonates. *Biochemistry.* 33:6840–6849. http://dx.doi.org/10.1021/bi00188a013

Wang, J., and E. London. 2009. The membrane topography of the diphtheria toxin T domain linked to the A chain reveals a transient transmembrane hairpin and potential translocation mechanisms. *Biochemistry.* 48:10446–10456. http://dx.doi.org/10.1021/bi9014665

Wilson, G.G., and A. Karlin. 1998. The location of the gate in the acetylcholine receptor channel. *Neuron.* 20:1269–1281. http://dx.doi.org/10.1016/S0896-6273(00)80506-1

Wonderlin, W.F., A. Finkel, and R.J. French. 1990. Optimizing planar lipid bilayer single-channel recordings for high resolution with rapid voltage steps. *Biophys. J.* 58:289–297. http://dx.doi.org/10.1016/S0006-3495(90)82376-6

Zhan, H., K.J. Oh, Y.-K. Shin, W.L. Hubbell, and R.J. Collier. 1995. Interaction of the isolated transmembrane domain of diphtheria toxin with membranes. *Biochemistry.* 34:4856–4863. http://dx.doi.org/10.1021/bi00014a043

Zhang, H., and A. Karlin. 1997. Identification of acetylcholine receptor channel-lining residues in the M1 segment of the β-subunit. *Biochemistry.* 36:15856–15864. http://dx.doi.org/10.1021/bi972357u

Zhao, G., and E. London. 2005. Behavior of diphtheria toxin T domain containing substitutions that block normal membrane insertion at Pro345 and Leu307: Control of deep membrane insertion and coupling between deep insertion of hydrophobic subdomains. *Biochemistry.* 44:4488–4498. http://dx.doi.org/10.1021/bi047705o